

# Selected Talks



- ST-A-01 In-cell NMR Spectroscopy of Proteins Using *Xenopus laevis* oocytes**  
*Hidehito Tochio, Tomomi Sakai, Kousuke Inomata, Ryuji Igarashi, Takahiro Iwazu, Ayako Ohno, Takeshi Tenno, Hidekazu Hiroaki, Masahiro Shirakawa*
- ST-A-02 Structure, Function and Evolution of  $\beta$ -thymosin/WH2 Actin-binding Domains**  
*Carine van Heijenoort, François-Xavier Cantrelle, Maud Hertzog, Dominique Didri, Louis Renault, Eric Guittet, Marie-France Carlier*
- ST-B-01  $^{13}\text{C}$  NMR of Methyl Iodide and Methane in Thermotropic Nematic Liquid Crystals Confined to Mesoporous Glasses**  
*Jukka Jokisaari, Pekka Tallavaara*
- ST-B-02 Structure Characterization of Fluoropolymers**  
*Ulrich Scheler, Salim Ok, Guido Pintacuda, Bénédicte Elena, Lyndon Emsley*
- ST-C-01 Investigation of Shear Banding Fluctuations in Wormlike Micelles Using Rapid NMR Velocimetry**  
*Kirk W. Feindel, María R. López-González, William M. Holmes, Paul T. Callaghan*
- ST-C-02 Novel MRI Contrast Enhancement by Active Radiation Damping Feedback**  
*Dennis W. Hwang, Susie Y. Huang, Chou-Hsiung Hsu, Yung-Ya Lin, Lian-Pin Hwang*
- ST-A-03 NMR Structural Dissection of the Human TFIIH Transcription and Repair Factor Using NMR**  
*Bruno Kieffer, Arnaud Poterszman, Marc Vitorino, Andrew Atkinson, Esther Kellenberger, Emeric Wasielewski, Virginie Gervais, Dino Moras, Jean-Marc Egly*
- ST-A-04 NMR Identification of Transient Complexes Critical to Adenylate Kinase Catalysis**  
*Magnus Wolf-Watz, Jörgen Ådén*
- ST-A-05 NMR Delineation of a Novel TAF31-Binding Motif within a Mostly Unstructured VP16 Transcriptional Activation Domain**  
*Seung-Wook Chi<sup>1</sup>, Do-Hyoung Kim, Si-Hyung Lee, Ki Hoon Nam, Kyou-Hoon Han*
- ST-A-06 Structural Characterization of the Thioredoxin-Thioredoxin Reductase Complex From *Saccharomyces cerevisiae***  
*Amorim G. C., Netto L. E. S., Valente A. P., Almeida F. C. L.*
- ST-B-03 The Solution Structure of the Adhesion Protein Bd37 from *Babesia* Divergens Reveals Structural Homology with Eukariotic Proteins Involved in Membrane Trafficking.**  
*Christian Roumestand, Stéphane Delbecq, Daniel Auguin, Yin-Shan Yang, Stefan Arold, Theo Schettlers, André Gorenflot*
- ST-B-04 Detection of Slow Conformational Transitions in D1 Domain of Human Annexin by Variable Pressure NMR**  
*Ryo Kitahara, Matthieu Gallopín, Erick Guittet, Kazuyuki Akasaka, Carine van Heijenoort*
- ST-B-05 Structure of a Eukaryotic, Mitochondrial Ion Channel by a Combination of Solution NMR and X-ray Crystallography – Structural and Functional Analysis of the Human Voltage Dependent Anion Channel (HVDAC)**  
*Monika Bayrhuber, Thomas Meins, Vinesh Vijayan, Clemens Vonrhein, Stefan Becker, Christian Griesinger, Kornelius Zeth, Markus Zweckstetter*
- ST-B-06 Caught in the Act: Solution Structure and Dynamics of Sortase A Transpeptidase Bound to Covalent Catalytic Intermediate**  
*Nuttee Suree, Mandar T. Naik, Chu Kong Liew, William Thieu, Jeremy J. Clemens, Michael E. Jung, Robert T. Clubb*
- ST-C-03 Metabonomics of *Caenorhabditis elegans* mutants by  $^1\text{H}$  High-Resolution Magic Angle Spinning Nuclear Magnetic Resonance Spectroscopy.**  
*Bénédicte Elena, Benjamin Blaise, Jean Giacomotto, Laurent Ségalat, Marc-Emmanuel Dumas, Lyndon Emsley.*
- ST-C-04 NMR, EPR, and Kinetic Studies of the Structure and Function of the Alzheimer's Disease-Related Metallo- $\beta$ -Amyloid**  
*Li-June Ming, Alexander Angerhofer, Giordano da Silva, and William Tay*
- ST-C-05 Mechanism of ligand uptake and release in insect pheromone binding proteins**  
*Fred F. Damberger, Erich Michel, Yuko Ishida, Walter S. Leal, Kurt Wuthrich*
- ST-C-06 Structural Basis for the Regulation of ASPP-Mediated Apoptosis of p53**  
*Jinwoo Ahn, In-Ja L. Byeon, Chang-Hyeock Byeon and Angela M. Gronenborn*
- ST-A-07  $^{19}\text{F}$  NMR Characterization of Hemoproteins Reconstituted with Fluorinated Hemes**  
*Yamamoto Yasuhiko*

- ST-A-08 The INPHARMA Method as a Novel and Powerful Tool for Pharmacophore Mapping**  
*Teresa Carlomagno, Julien Orts, Marcel Reese, Jennifer Tuma, Christian Griesinger*
- ST-B-07 Local Structures and Dynamics of Phorbodopsin and Transducer Leading to Signal Transduction as Revealed by Site-Directed Solid State <sup>13</sup>C NMR**  
*Akira Naito, Izuru Kawamura, Hideaki Yoshida, Yoichi Ikeda, Satoru Yamaguchi, Satoru Tuzi, Naoki Kamo, Hazime Saito*
- ST-B-08 Solid-State NMR Studies of the Structure and Dynamics of Membrane Bound Ras Proteins**  
*Daniel Huster, Guido Reuther, Alexander Vogel, Kui-Thong Tan, Christine Nowak, Jürgen Kuhlmann, Herbert Waldmann*
- ST-C-07 EPR Mapping of Inhibitor Binding Sites on Enzymes**  
*Betty J. Gaffney, Fayi Wu*
- ST-C-08 Multifrequency EPR Lineshape Analyses on Biradicals for High-Frequency Dynamic Nuclear Polarization**  
*Kan-Nian Hu, Changsik Song, Hsiao-hua Yu, Timothy M. Swager, Robert G. Griffin*
- ST-A-09 Large Pictures with Small Details: Combined Use of NMR and Scattering Data for RNA Structure Determination**  
*Y-X. Wang, X. Zuo, J. Wang, P. Yu, C. Schwieters*
- ST-A-10 Studies on the SARS coronavirus nucleocapsid protein using a hybrid approach – From structure to function**  
*Chung-ke Chang, Yuan-hsiang Chang, Yen-lan Hsu, Chun-Yuan Chen, Ming-Chya Wu, Chin-Kun Hu, Chwan-Deng Hsiao, Tai-huang Huang\**
- ST-B-09 Probing Amide Bond Nitrogens in Solids using <sup>14</sup>N NMR Spectroscopy**  
*Sasa Antonijevic, Nicholas Halpern-Manners*
- ST-B-10 An in situ Solid State NMR Technique at Cryogenic Temperature**  
*Mingcan Xu, Kenneth D.M. Harris, John Meurig Thomas, David E.W. Vaughan*
- ST-C-09 Spatial Effects in the Localised Detection of Coupled Metabolites In Vivo**  
*Richard AE Edden, Peter B Barker*
- ST-C-10 Tract-Specific Analysis of Human White Matter: Mean-Path Based Method**  
*W.-Y. Chiang\*, H.-L. Wang, S.-C. Huang, F.-C. Yeh, W.-Y. Tseng*
- ST-A-11 Fast and Automated Assignment of (<sup>1</sup>H-<sup>15</sup>N) Amide Resonances of Proteins of Known 3D-structure.**  
*Eric Guittet\*, Dirk Stratmann, Carine van Heijenoort*
- ST-A-12 Automated NMR Structure Determination**  
*Torsten Herrmann, Pascal Bettendorff, Francesco Fiorito, Jochen Volk, Kurt Wüthrich*
- ST-B-11 Structural and Functional Polymorphism of Chromodomains from Chromatin Remodeling Factors**  
*Yoshifumi Nishimura, Masahiko Okuda, Hideaki Shimojoi, Masami Horikoshi*
- ST-B-12 Solution Structures of DNA Duplexes Containing Oxidative Cytosine Lesions and Their Removal by DNA Glycosylases**  
*Varatharasa Thiviyanathan, Anoma Somasunderam, David Volk Tapas Hazra, David Gorenstein*
- ST-C-11 Quantum Oscillations in Photo-excited Triplet States in an External Magnetic Field**  
*Gerd Kothe, Tomoaki Yago, Michail Lukaschek, Jörg-Ulrich Weidner, Gerhard Link, David J. Sloop, Tien-Sung Lin*
- ST-C-12 A Low Temperature X-band Probe Head for Decoherence Time Study of Semiconductors**  
*N. Suwuntanasarn, W. D. Hutchison, G. Milford, R. Bramley*
- ST-A-13 Alpha Hemoglobin Stabilizing Protein Sets a Conformational Trap to Stabilize Alpha Hemoglobin**  
*Joel P Mackay, David A Gell, Liang Feng, Suiping Zhou, Mitchell J. Weiss, Yigong Shi*
- ST-A-14 Protein Folding and ssDNA Binding of Cold-shock Protein CspB Studied on a nano-to-millisecond time**  
*Jochen Balbach*

- ST-A-15 Kinetic and Equilibrium Intermediate Structures in Globin Proteins**  
*Chiaki Nishimura, H. Jane Dyson, and Peter E. Wright*
- ST-A-16 Structural Basis of Phosphor-counting Switch for Sequential Activation of a Checkpoint Kinase Cascade**  
*Chunhua Yuan, Hyun Lee, Andrew Hammet, Anjali Mahajan Chi-Fon Chang, Jörg Heierhorst, Ming-Daw Tsai*
- ST-B-13 High Resolution Solid-State  $^1\text{H}$ - $^{15}\text{N}$  HETCOR Spectroscopy for Structural Characterization of Multiply-Labeled Peptides in Aligned Bilayers**  
*Riqiang Fu, Milton Truong, Randy J. Saager, Breanna S. Vollmar, Timothy A. Cross, Myriam Cotten*
- ST-B-14 Backbone Assignments in Solid-State Proteins using J – Based 3D Heteronuclear Correlation Spectroscopy**  
*Leonard J. Mueller, Lingling Chen,<sup>1</sup>J. Michael Kaiser, Tatyana Polenova, Jun Yang,<sup>2</sup>Chad M. Rienstra,*
- ST-B-15 Enzyme Activation in Organic Solvents: Water Dynamics, Enzyme Dynamics, and Active Site Polarity via Solid-state NMR**  
*Jeffrey A Reimer, Ross K. Eppler, Douglas S. Clark*
- ST-B-16 Chemical Shift Analysis and Structural Studies of Human  $\alpha$ -B Crystallin by MAS Solid-state NMR**  
*Stefan Jehle, Ponni Rajagopal, Hartmut Oschkinat, Barth-Jan van Rossum*
- ST-C-13 Enhancement of Spin Diffusion of Quadrupolar Spins in Solids under Magic-Angle-Spinning**  
*Shangwu Ding, Po-Chi Huang*
- ST-C-14 MRI Signal Enhancement in Rodent Brain by Pulmonary Infusion of  $\text{MnCl}_2$**   
*Kyuhong Lee, Hye-Young Moon, Hong-il Lee, Chaejoon Cheong, Kwan Soo Hong*
- ST-C-15  $^{13}\text{CO}_2$  labeling into plant biomass and its bacterial degradation followed by solution and solid-state NMR**  
*Jun Kikuchi, Tetsuya Mori, Masahiro Yuki, and Takashi Hirayama*
- ST-C-16 Study of Long-Term Stability of Yttrium-Iron Garnet Films under Irradiation by Reactor Neutrons**  
*V. A. Ageev, V. I. Kirischuk, Yu. V. Koblyanskiy, G. A. Melkov, L. V. Sadovnikov, N. V. Strilchuk, V. A. Zheltonozhsky*

**Oct. 15, 11:45~12:15**

**ST-A-01**

### **In-cell NMR Spectroscopy of Proteins Using *Xenopus laevis* oocytes**

Hidehito Tochio<sup>1</sup>, Tomomi Saka<sup>2</sup>, Kousuke Inomata<sup>1</sup>, Ryuji Igarashi<sup>1</sup>, Takahiro Iwazu<sup>1</sup>, Ayako Ohno<sup>1</sup>, Takeshi Tenno<sup>3</sup>, Hidekazu Hiroaki<sup>3</sup>, Masahiro Shirakawa<sup>1</sup>

<sup>1</sup> Graduate School of Engineering, Kyoto University, Kyoto, 615-8510, Japan; <sup>2</sup> International Graduate School of Arts and Sciences, Yokohama City University, Yokohama, 230-0045, Japan; <sup>3</sup> Department of Biochemistry and Molecular Biology, Graduate School of Medicine, Kobe University

In-cell NMR is a method for analysis of proteins inside living cells, and has been successfully applied for bacterial cells by selective labeling of proteins over-expressed in the cells. In order to monitor conformation and function of proteins inside vertebrate cells, we have measured high-resolution NMR spectra of labeled proteins micro-injected to oocytes from *Xenopus laevis*.

The two-dimensional <sup>1</sup>H, <sup>15</sup>N-correlation spectra of the wild-type ubiquitin inside oocytes displayed rather fewer and weaker cross peaks than that of a ubiquitin derivative harboring substitutions of residues that form the presumed interfacial surface for downstream ubiquitin-interacting proteins. The in-cell NMR spectra of a series of ubiquitin derivatives suggest that protein-protein interactions between ubiquitin and endogenous ubiquitin-binding proteins in the oocytes cause signal broadening.

We also observed the cleavage of the C-terminal residue of one of the ubiquitin derivatives, which mimics ubiquitin precursor, by endogenous ubiquitin maturation enzymes, such as ubiquitin C-terminal hydrolase (UCH). This cleavage was partly suppressed by the pre-injection of ubiquitin aldehyde, an inhibitor of UCH activity. Under this condition, the cleavage reaction was monitored by a series of in-cell NMR spectra.

**ST-A-02**

### **Structure, Function and Evolution of $\beta$ -thymosin/WH2 Actin-binding Domains**

François-Xavier Cantrelle<sup>1</sup>, Maud Hertzog<sup>2</sup>, Dominique Didr<sup>2</sup>, Louis Renault<sup>2</sup>, Eric Guittet<sup>1</sup>, Marie-France Carlier<sup>2</sup> and Carine van Heijenoort<sup>1\*</sup>

<sup>1</sup>ICSN, <sup>2</sup>LEBS, CNRS, Gif-sur-Yvette.

The conserved WH2 module has been identified in a large number of proteins that all interact with actin. The functional evolution of the WH2 domain was approached by a combination of structural and biochemical methods, using thymosin  $\beta$ 4 and Ciboulot, a 3  $\beta$ -thymosin repeat protein as models. The first repeat of Ciboulot (D1) promotes actin self-assembly whereas T $\beta$ 4 inhibits it. The versatile functions of WH2 modules may be linked to changes in the actin-WH2 interface, leading to promotion or inhibition of actin self-assembly. NMR studies show that T $\beta$ 4 and D1 are largely unfolded in solution and that their binding to G-actin is coupled with a complete folding of the whole domains [1]. Further NMR and XRay analyses suggested that the functional switch from inhibition to promotion of actin assembly was linked to disparities in the dynamics of interaction of the central and C-terminal regions of WH2 domains with G-actin, allowing or not the pointed face of actin in the complex to interact with a filament barbed end [2]. A series of chimeras of Ciboulot and T $\beta$ 4 were engineered in order to evaluate the contributions of the different regions of these two proteins in the biological function and in the crystal and solution structures of their complex with actin [3]. Proteins displaying either promotion function or enhanced sequestering activity as compared to T $\beta$ 4 have been obtained and characterized. The results provide insight into the structural basis for the regulation of the multiple functions of the WH2 domain.

[1] Domanski et al (2004) J. Biol. Chem. **279**:23637,

[2] Hertzog et al. (2004) Cell **117**:611,

[3] Carlier et al. (2007) Annals of the New York Academy of Science (in process).

## **<sup>13</sup>C NMR of Methyl Iodide and Methane in Thermotropic Nematic Liquid Crystals Confined to Mesoporous Glasses**

*Jukka Jokisaari and Pekka Tallavaara*

*Department of Physical Sciences, University of Oulu, 90014 Oulu, Finland*

The behavior of thermotropic liquid crystals (LCs) confined to mesoporous controlled pore glasses (CPG) was investigated using <sup>13</sup>C NMR spectroscopy of methyl iodide and methane used as probe molecules. The average pore diameters of the materials varied from 81 to 375 Å, and the temperature series measurements were performed on solid, nematic and isotropic phases of bulk LCs. Chemical shift, intensity and line shape analyses of the resonance signals in the spectra yield information about the effect of confinement on the state of the LCs. The line shape of the <sup>13</sup>C resonances of the CH<sub>3</sub>I molecules appeared to be very sensitive to the LC orientation distribution. The effect of the magnetic field on the orientation of LC molecules inside the pores was examined in four magnetic fields varying from 4.70 to 11.74 T. Magnetic field was found to have significant effect on the orientation of LC molecules in the largest pores and close to nematic-isotropic phase transition temperature. <sup>13</sup>C powder pattern spectrum of CH<sub>3</sub>I was modeled in terms of the <sup>13</sup>C shielding anisotropy, degree of molecular order, direct <sup>1</sup>H-<sup>13</sup>C dipole-dipole and indirect <sup>1</sup>H-<sup>13</sup>C spin-spin coupling constant.

The system described above offers also a novel NMR method for determining nuclear shielding anisotropies in molecules. As an example, the <sup>13</sup>C shielding tensor anisotropy,  $\Delta\sigma_C$ , of methyl iodide was determined at variable temperatures. The method is based on the facts that (a) methyl iodide molecules experience on average isotropic environment in LCs inside the smallest pores, and (b) in the spaces in between the CPG particles LCs behave like in bulk, leading to anisotropic orientation distribution. Consequently, isotropic values of the shielding tensor can be determined from the spectra arising from molecules inside the pores at exactly the same temperature as the anisotropic ones from molecules outside the pores.

## **Structure Characterization of Fluoropolymers**

*Salim Ok, Guido Pintacuda, Bénédicte Elena, Lyndon Emsley, Ulrich Scheler*

*Leibniz Institute of Polymer Research Dresden, Hohe Str. 6, D-01069 Dresden, Germany. ENS Lyon, 46 allée d'Italie, Lyon Cedex 07, France*

<sup>19</sup>F is the ideal probe nucleus for the characterization of fluoropolymers because of its high receptivity and the large chemical shift range. Distance information is available through the direct dipolar coupling, which can be utilized for the assignments of the chemical shifts to fine structures. The RFDR experiment is very robust and provides a wealth of information on internuclear proximity. Additional information is available from double quantum experiments, where the strong signals from CF<sub>2</sub> groups often becomes a problem. Additional information particularly in partially fluorinated materials is obtained from <sup>13</sup>C spectra. In that case dedicated heteronuclear decoupling sequences are required. Broadband <sup>19</sup>F decoupling is achieved by fast adiabatic pulses. If simultaneous proton decoupling has to be applied. Interference of the time evolutions of the two decoupling sequences has to be avoided.

The direct dipolar coupling between abundant fluorines is not completely averaged by fast MAS and additional line narrowing is required. The usual homonuclear and heteronuclear decoupling techniques are difficult because of their limited bandwidth. New approaches based on adiabatic pulses are demonstrated. For structure assignment better resolution is obtained in high-temperature NMR in melts and of fluoropolymers dissolved in supercritical CO<sub>2</sub>. Solution-NMR type experiments like NOESY and TOCSY are applied drastically improving signal assignments and thus permitting the investigation of triads in the copolymer chain structure.

Ultimately these information is utilized in the understanding of solid-state spectra for the characterization of packing effects and phase separation in the semicrystalline polymers.

Applications include perfluorinated and partially fluorinated polymers and polycrystalline model compounds. Examples will be give for the structural assignments. Additional information is available from high-temperature NMR of the polymer melts, where better resolution can be achieved.

## Investigation of Shear Banding Fluctuations in Wormlike Micelles Using Rapid NMR Velocimetry

Kirk W. Feindel<sup>1</sup>, María R. López-González<sup>1</sup>, William M. Holmes<sup>2</sup>, Paul T. Callaghan<sup>1</sup>

<sup>1</sup>MacDiarmid Institute, Victoria University of Wellington, Wellington, New Zealand, <sup>2</sup>Wellcome Surgical Institute, University of Glasgow, Glasgow, United Kingdom

Whilst the macroscopic behaviour of complex fluids is often readily observable, the flow and deformational (i.e., rheological) properties and their molecular origin are, in general, not well understood. One of the objectives of our research is to improve the understanding of complex fluids via experimental investigation of model systems, such as solutions of wormlike micelles. The flow curves of shear-thinning wormlike micellar systems, above a critical shear rate often exhibit a stress plateau which has been associated with the spatial separation of the system into regions of differing local shear rate, a phenomenon termed shear banding.

By combining conventional rheological methodology with magnetic resonance techniques (rheo-NMR), previously elusive information about the properties and behaviour of complex fluids can be garnered. The model system investigated here is a shear-thinning solution of 10 w/w% cetylpyridinium chloride and sodium salicylate in 0.5 M NaCl (far from the isotropic-to-nematic phase transition).

We present results that highlight our recent progress in the development of rapid NMR velocimetry techniques for real-time investigations of shear banding fluctuations in wormlike micelle solutions. Rheo-NMR experiments were conducted using a 9.4 T vertical wide-bore superconducting magnet, Bruker Avance 400 console, and a Bruker microimaging accessory. Steady shear deformation was performed using a Rheo-NMR system and a custom Couette cell. We have developed rapid 2D slice selective EPI- and RARE-type imaging sequences that are preceded by a PGSE encoding period to yield 2D velocity maps. We also present our results from preliminary experiments that investigate velocity fluctuations along the vorticity direction of the Couette cell gap.

## Novel MRI Contrast Enhancement by Active Radiation Damping Feedback

Dennis W. Hwang<sup>1,2</sup>, Susie Y. Huang<sup>3</sup>, Chou-Hsiung Hsu<sup>1</sup>, Yung-Ya Lin<sup>3</sup>, Lian-Pin Hwang<sup>1,4,\*</sup>

<sup>1</sup>Department of Chemistry, National Taiwan University, Taipei, Taiwan, <sup>2</sup>Department of Radiology, National Taiwan University Hospital, Taipei, Taiwan, <sup>3</sup>Department of Chemistry and Biochemistry, University of California, Los Angeles, USA, <sup>4</sup>IAMS, Academia Sinica, Taiwan

MRI is one of the most important noninvasive methods in modern clinical diagnosis, and contrast improvement is a crucial issue. Feedback fields such as radiation damping (RD) have demonstrated their potential in contrast enhancement and highlighting structures not visible in conventional imaging. Nevertheless, for most MR spectrometers/scanners, the sensitivity and quality factor of the RF receiver coil is not high enough to induce a strong RD field. Utilizing an external electronic device can significantly enhance the RD feedback field.

In this work, we demonstrate an active RF feedback loop [Fig. 1] to amplify and control the RD feedback field. To validate the efficacy of active RF feedback, tumor detection in *in vivo* mice was investigated. The mice were injected subcutaneously with human lung cell line. The sample was first excited by a single-shot hard pulse, followed by evolution under active RD feedback. The sample was then imaged by conventional spin-echo imaging. The resulting active RD feedback-enhanced image showed strong contrast and highlighted boundaries in an early stage tumor [Fig. 2(b)]. These features were barely distinct in the corresponding conventional proton density,  $T_1$ -weighted,  $T_2$ -weighted, and  $T_2^*$ -weighted images [Figs. 2(a), (c)-(e), respectively]. Moreover, the tumor size observed in the active RD feedback-enhanced image was consistent with that measured by the histology [Fig. 2(f)]. Figure 3 demonstrates another advantage of active RD feedback-enhanced images. In comparison with the optical image [Fig. 3(a)], active RD feedback-enhanced image can clearly indicate more detailed tumor structure [Fig. 3(b)] which cannot be distinguished by conventional image, such as  $T_2$ -weighted image [Fig. 3(c)].

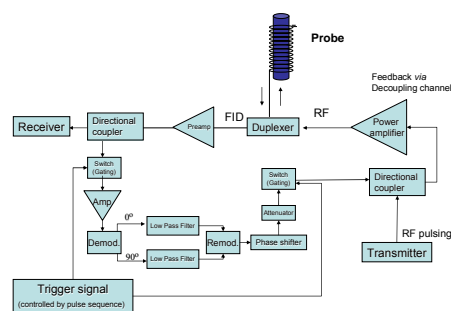


Figure 1. Block diagram of active radiation damping feedback circuit

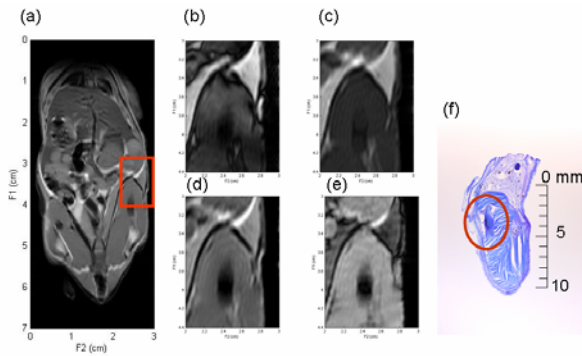


Figure 2. Tumor of mice *in vivo*. (a) Proton density image. (b) Active feedback-enhanced image. (c) T<sub>1</sub>-weighted image (d) T<sub>2</sub>-weighted image. (e) T<sub>2</sub>\*-weighted image. (f) Histology.

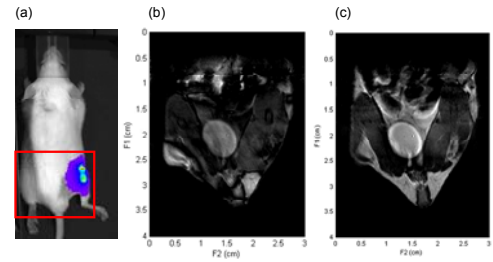


Figure 3. Tumor of mice *in vivo*. (a) GFP expressing optical image. (b) Active feedback-enhanced image. (c) T<sub>2</sub>-weighted image.

In summary, differential excitation under the feedback field distinguishes tissues and enhances contrast at the tissue boundaries, especially for abnormal tissues, e.g. tumor. The development of an active feedback circuit to amplify the RD field thus enables improved differentiation of neighboring normal and abnormal tissues at low fields using conventional probes/receiver coils.

**Oct.15 15:10~16:10**

**ST-A-03**

### **NMR Structural Dissection of the Human TFIIH Transcription and Repair Factor Using NMR**

*Arnaud Poterszman<sup>1</sup>, Marc Vitorino<sup>1</sup>, Andrew Atkinson<sup>1</sup>, Esther Kellenberger<sup>1</sup>, Emeric Wasielewski<sup>1</sup>, Virginie Gervais<sup>1</sup>, Dino Moras<sup>1</sup>, Jean-Marc Egly<sup>1</sup>, Bruno Kieffer<sup>1,\*</sup>*

<sup>1</sup>IGBMC, Illkirch France

Transcription initiation and nucleotide excision repair (NER) of damaged DNA are connected through the dual action of TFIIH, a multiprotein complex (460 kDa) composed of ten subunits. Mutations in the the two helicases subunits result in DNA repair defects leading to xeroderma pigmentosum (XP), Cockayne syndrome (CS) or trichothiodystrophy (TTD) phenotypes. The combined use of proteolysis experiments and bioinformatics allowed the identification of several structural domains in TFIIH subunits that could be studied in solution using NMR. The three-dimensional structure of two domains related to the repair activity of TFIIH will be presented. The first one is a PH/PTB domain that is found within the p62 subunit. We showed that the p62 PH/PTB-like domain is dispensable for the assembly of the TFIIH complex and basal transcription. Instead dual incision experiments revealed that the p62 PH/PTB-like domain is required for nucleotide excision repair and physically interacts with the 3' endonuclease XPG. Thus, our study provides an example of a PH/PTB-like domain potentially involved in the shuttling of TFIIH between NER and transcription enlarging the repertory of interactions mediated by PH/PTB domains. Recently, the role of the smallest TFIIH subunit in trichothiodystrophy (TTD-A) was reported. The solution structure of this subunit reveals the presence of a dimer. Mutagenesis studies coupled to Biophysical investigations were undertaken and shed light on the structural basis of TTD-A disease.

**ST-A-04**

### **NMR Identification of Transient Complexes Critical to Adenylate Kinase Catalysis**

*Jörgen Ådén, Magnus Wolf-Watz<sup>1</sup>*

<sup>1</sup>Department of Chemistry, University of Umeå, Sweden

A fundamental question in protein chemistry today is how the native energy landscape of enzymes can enable efficient catalysis of chemical reactions. Adenylate kinase is a small monomeric enzyme that catalyzes the reversible interconversion of AMP and ATP into two ADP molecules. Previous structural studies have revealed that substrate binding is accompanied by large rate-limiting spatial displacements of

both the ATP and AMP binding motifs. We present a solution state NMR approach to probe the native energy landscape of adenylate kinase in its free form, and in complex with its natural substrates and in presence of a tight binding inhibitor. Binding of ATP induces a dynamic equilibrium in which the ATP binding motif populates both open and closed conformations with almost equal weights. A similar scenario is observed for AMP binding that induces an equilibrium between open and closed conformations for the AMP binding motif. These ATP and AMP bound structural ensembles represent complexes that are populated transiently during the enzymatic reaction cycle. Simultaneous binding of AMP and ATP is required to force both substrate binding motifs to close cooperatively enabling the chemical step to occur. In addition a previously unknown unidirectional energetic coupling between the ATP and AMP binding sites was discovered, suggesting that adenylate kinase is an allosteric enzyme. Based on these and previous results we propose that adenylate kinase belongs to a group of enzymes whose substrates acts to shift preexisting equilibria towards catalytically active states.

**ST-A-05**

### **NMR Delineation of a Novel TAF31-Binding Motif within a Mostly Unstructured VP16 Transcriptional Activation Domain**

Seung-Wook Chi<sup>1</sup>, Do-Hyoung Kim<sup>1</sup>, Si-Hyung Lee<sup>1</sup>, Ki Hoon Nam<sup>1</sup>, Kyou-Hoon Han<sup>1,\*</sup>

<sup>1</sup>Molecular Cancer Research Center, Korea Research Institute of Bioscience and Biotechnology, Yusong, Daejeon, 305-806, Korea

Transcriptional activation domain (TAD) in virion protein 16 of herpes simplex virus is intrinsically unstructured, yet exhibits a potent transcriptional activity. We have used NMR spectroscopy to investigate structural features of VP16 TAD in a target-unbound and a TAF31-bound state. Results show that, while mostly unstructured, the target-unbound VP16 TAD has three regions (residues 424-433, 442-446 and 472-479) that show transient structural order and exhibit different dynamic behavior from the rest of the molecule. Multiple transiently pre-structured motifs have been observed in other target-unbound TADs and found to be functionally critical. Upon binding to human TFIID TATA box-binding protein-associated factor 31 (TAF31), VP16 TAD experiences NMR chemical shift perturbations significantly at residues 423-428 and 432-439, and to a less degree at 462-484. The residues 472-483 in VP16 TAD were previously identified as a TAF31-binding region (Uesugi, M., Nyanguile, O., Lu, H. Levine, A. J., and Verdine, G. L. (1997) *Science* 277, 1310-1313). Thus, the region encompassing residues 423-439 in VP16 TAD is a novel TAF31-binding motif that has a stronger TAF31-binding ability than the known. The pre-structured motifs delineated here overlap partially with the regions interacting with a human transcriptional coactivator positive cofactor (PC4) or a general transcription factor TFIIB. Taken together, these results concur with a notion that such pre-structured motifs in mostly unstructured proteins guide binding of diverse target proteins to TADs.

**ST-A-06**

### **Structural Characterization of the Thioredoxin-Thioredoxin Reductase Complex From *Saccharomyces cerevisiae***

Amorim G. C.<sup>1</sup>, Netto L. E. S.<sup>2</sup>, Valente A. P.<sup>1</sup> and Almeida F. C. L.<sup>1</sup>

<sup>1</sup>Centro Nacional de Ressonância Magnética Nuclear - IBqM - CCS - UFRJ - Rio de Janeiro – RJ, <sup>2</sup>Instituto de Biociências - Universidade de São Paulo - São Paulo – SP

Thioredoxin system – thioredoxin (Trx), thioredoxin reductase (TrR) and NADPH – is an ubiquitous oxidoreductive (dithiol-disulfide) system important for cellular defense against oxidative stress. In yeast, it has been described two cytosolic thioredoxins (Trx1 and Trx2) and one cytosolic thioredoxin reductase (TrR1). TrR is composed by two domains, and each of them has a NADPH or a FADH non-covalently attached. Two different structures have been determined for *E. coli* TrR, one in the FO (open) conformation and another, bound to Trx, in the FR (close). Our aim is to get insights into the structure and dynamics of Trx-TrR complexes from *Saccharomyces cerevisiae*, investigating structural requirements for the interaction. We determined the solution structure of Trx1 and Trx2 and studied by NMR the binding of Trxs to TrR1. We mapped the binding by analyzing chemical shift perturbations and line broadening. The

chemical shift difference revealed that Trxs oxidized structure is very similar to bound Trxs. Showing that oxidized Trxs are structurally ready to bind to TrR. We also characterized the structural behavior of TrR1 under complex formation. In the presence of Trxs a flavin-thiolate charge transfer complex is stabilized. ITC experiments showed that, in the presence of 10 mM DTT, the enzyme is not totally reduced and a chemical reaction is occurring. Only in the presence of 50 mM of sodium dithionite, where the enzyme is totally reduced, we can measure binding parameters. FRET data indicates that the binding of Trxs to TrR1 induces the release of the NADPH cofactor. In yeast cell, the equilibrium may be shifted to the FR conformation due to the high cytosolic concentration of Trxs.

Acknowledgements: CNPq, FINEP, FAPERJ, Millenium Institute of Structural Biology, Biomedicine and Biotechnology.

### ST-B-03

#### The Solution Structure of the Adhesion Protein Bd37 from *Babesia Divergens* Reveals Structural Homology with Eukaryotic Proteins Involved in Membrane Trafficking.

Stéphane Delbecq<sup>2</sup>, Daniel Auguin<sup>1</sup>, Yin-Shan Yang<sup>1</sup>, Stefan Arold<sup>1</sup>, Theo Schettters<sup>3</sup>, André Gorenflo<sup>2</sup>, and Christian Roumestand<sup>1</sup>.

<sup>1</sup>CNRS, UMR5048, Centre de Biochimie Structurale, F34090 Montpellier, France ; INSERM, U554, F34090 Montpellier, France ; Université Montpellier 1 et 2, F34090 Montpellier, France, <sup>2</sup> DINMP, Université de Montpellier I et II, CNRS, Laboratoire de Biologie Cellulaire et Moléculaire, ERT 1038, Faculté de Pharmacie BP 14491, 15 Avenue Charles Flahault, 34093 Montpellier Cedex 5, France, <sup>3</sup> Department of Parasitology, Intervet International B.V., Boxmeer, The Netherlands.

*Babesia divergens* is the Apicomplexa agent of the bovine babesiosis in Europe: this infection leads to growth and lactation decrease, so that economical losses due to this parasite are sufficient to require the development of a vaccine. The major surface antigen of *Babesia divergens* has been described as a 37 kDa protein GPI-anchored at the surface of the merozoite. The immuno-prophylactic potential of Bd37 has been already demonstrated, and we present here the high resolution solution structure of the 27 kDa structured core of Bd37 ( $\Delta$ -Bd37) using NMR spectroscopy. A model for the whole protein has been obtained using additional SAXS data. The knowledge of the 3D structure of Bd37 allowed the precise epitope mapping of antibodies on its surface. Interestingly, the geometry of  $\Delta$ -Bd37 reveals an intriguing similarity with the exocyst subunit Exo84p C-terminal region, an eukaryotic protein that has a direct implication in vesicle trafficking. This strongly suggest that Apicomplexa have developed in parallel molecular machines similar in structure and function than the ones used for endo- and exocytosis in eukaryotic cells.

### ST-B-04

#### Detection of Slow Conformational Transitions in D1 Domain of Human Annexin by Variable Pressure NMR

Ryo Kitahara<sup>1</sup>, Matthieu Gallopin<sup>2</sup>, Erick Guittet<sup>2</sup>, Kazuyuki Akasaka<sup>3</sup> and Carine van Heijenoort<sup>2</sup>

<sup>1</sup>RIKEN SPring-8 Center, Japan, <sup>2</sup>CNRS-ICSN, Gif-syr-Yvette, France, <sup>3</sup>Kinki University, Japan

We examined dynamics of D1 domain of human annexin 1 (A1D1, 81 residues) by utilizing the variable pressure NMR spectroscopy. <sup>15</sup>N/<sup>1</sup>H HSQC measurements have done between 1 and 3000 bar at 500 MHz and 800 MHz (293K, pH 4.4). Interestingly, several cross-peaks were broadened, then split into two in the nitrogen axis with increasing pressure (e.g. res71 in Figure 1A and B). This observation shows a presence of the chemical exchange process between two different conformational states on these residue sites, and reflects a decrease in the exchange rates with increasing pressure. The cross-peak splitting provides a number of the exchanging states, chemical shifts ( $\omega_1$  and  $\omega_2$ ) and relative population of the states. Interestingly, extrapolation of  $\Delta\omega_N$  values to 1 bar gives  $\Delta\omega_N$  values very close to those from the <sup>15</sup>N relaxation dispersion NMR study at 1 bar. If we take the present information (the number and populations of the conformational states and  $\Delta\omega_N$ ) for <sup>15</sup>N relaxation dispersion data analysis, we would have more reliable fitting of the parameters ( $k_{AB}$ ,  $k_{BA}$ ,  $R_{ex}$ ) (e.g. res71,  $p_A=57\%$ ,  $p_B=43\%$ ,  $\Delta\omega_N=1.29$  ppm  $\rightarrow R_{ex}=54$  Hz,  $k_{AB}=630$  Hz,

$k_{BA}=830$  Hz,  $\tau_{ex}=0.68$  ms). In addition, broadening and splitting of cross-peaks were observed for many residues in the proton axis under high pressures (e.g. res61 in Figure 1A). It would be attributed to two different sidechain conformations of Tyr52. The present study showed that the conformational transition of the domain was clearly detected as NMR measurements were carried out under pressure. It is considered that pressure significantly retards the conformational transition of the domain because pressure increases the relative population of the semi-stable conformation and the activation volume is positive for the transitions. Therefore, in general, the detection of intermediate-to-slow time scale motions in proteins would become much easier with increasing pressure.

ST-B-05

### **Structure of a Eukaryotic, Mitochondrial Ion Channel by a Combination of Solution NMR and X-ray Crystallography – Structural and Functional Analysis of the Human Voltage Dependent Anion Channel (HVDAC)**

*Monika Bayrhuber*<sup>1</sup>, *Thomas Meins*<sup>2</sup>, *Vinesh Vijayan*<sup>1</sup>, *Clemens Vonrhein*<sup>3</sup>, *Stefan Becker*<sup>1</sup>, *Christian Griesinger*<sup>1</sup>, *Kornelius Zeth*<sup>4</sup>, *Markus Zweckstetter*<sup>1</sup>

<sup>1</sup>Max-Planck-Institute for Biophysical Chemistry, Göttingen, Germany; <sup>2</sup>Max-Planck-Institute for Biochemistry, Munich, Germany; <sup>3</sup>Global Phasing Ltd., Cambridge, UK; <sup>4</sup>Max-Planck-Institute for Developmental Biology, Tübingen, Germany

The human voltage dependent anion channel (HVDAC) is located in the outer mitochondrial membrane. It is primarily responsible for metabolite flux through the mitochondria. In this study the structure of HVDAC was determined conjointly by NMR-spectroscopy and X-ray crystallography. It is the first structure of a human, mitochondrial ion channel. HVDAC adopts a  $\beta$ -barrel fold. The N-terminal part, which contains the voltage-sensing domain, shows in solution an increased flexibility. The C-terminal part is mainly responsible for binding of interaction partners. The pro-apoptotic protein Bid and the anti-apoptotic protein Bcl-x<sub>L</sub> are interacting with the same site in the C-terminal part of HVDAC. The binding surface of Bid and HVDAC was established by chemical shift perturbations in the 15N TROSY-HSQC spectrum of HVDAC in the presence of a four-fold excess of Bid. Additionally paramagnetic labelled Bid was utilized to derive an extended binding interface based on PRE data. The lanthanide Gadolinium binds to the same site as Bid and Bcl-x<sub>L</sub>, close to the Ca<sup>2+</sup> binding site known from literature. This points out that apoptosis related factors compete for the same binding site in HVDAC. The antidepressant fluoxetine interacts mainly with a C-terminal loop that is not affected by apoptotic factors. Fluoxetine, like Bid, stabilises the low conducting state of HVDAC. Since the interaction sites of both molecules are not the same this indicates a different mechanism of channel closure. ADP interacts with low affinity with HVDAC and the binding sites distributed over the whole sequence. This is in line with nucleotide conductivity of HVDAC. The nucleotides should not bind tightly to the channel, but rather pass through it quickly.

ST-B-06

### **Caught in the Act: Solution Structure and Dynamics of Sortase A Transpeptidase Bound to Covalent Catalytic Intermediate**

*Nuttee Suree*, *Mandar T. Naik*, *Chu Kong Liew*, *William Thieu*, *Jeremy J. Clemens*, *Michael E. Jung*, and *Robert T. Clubb*

Department of Chemistry and Biochemistry, University of California, Los Angeles, 405 Hilgard Avenue, Los Angeles, CA 90095-1570, USA

*Staphylococcus aureus* is the leading cause of hospital-acquired infections in the United States and has become resistant to the available antibiotics, raising the need for new drugs. Here we present structural studies by NMR and inhibitor discovery of a new target enzyme called sortase A (SrtA), a transpeptidase in gram-positive bacteria that anchors surface proteins to the cell wall peptidoglycan unit. SrtA is highly conserved and critical for achieving bacterial virulence. Sortase inhibitors may function as anti-infective agents in gram-positive bacteria without affecting microbial viability. The process by which SrtA anchors a polypeptide, recognizing a sorting signal "LPXTG", to the peptidoglycan has been extensively studied. However, the exact mechanism of how SrtA recognizes its substrates remained unclear. Detailed structural studies of SrtA-substrate complexes have been hindered because of the low affinity of these interactions.

We have overcome this problem by determining the solution structure of a covalent SrtA-peptide complex that mimics the first thioacyl intermediate of catalysis. For the first time, this complex structure, supplemented by computational modeling studies, has revealed how the sorting signal is recognized. Additionally, we have identified a calcium binding site on SrtA and have performed detailed nitrogen-15 relaxation measurements, which allowed us to gain insight into how SrtA is allosterically regulated by this ion. The structural and dynamics data have shed light onto how sortase enzymes anchor proteins containing conserved LPXTG sorting signals, and has facilitated the design of therapeutically useful inhibitors of this enzyme class. By using a rational inhibitor design strategy, as well as high-throughput screening, we have identified several compounds that inhibit SrtA with high potency. A structure activity relationship (SAR) analysis has been performed on these lead compounds in order to optimize their potency.

ST-C-03

### Metabonomics of *Caenorhabditis elegans* mutants by <sup>1</sup>H High-Resolution Magic Angle Spinning Nuclear Magnetic Resonance Spectroscopy.

Benjamin Blaise<sup>1</sup>, Bénédicte Elena<sup>1</sup>, Jean Giacomotto<sup>2</sup>, Laurent Ségalat<sup>2</sup>, Marc-Emmanuel Dumas<sup>1</sup>, Lyndon Emsley<sup>1</sup>.

<sup>1</sup>Laboratoire de Chimie, UMR 5182 CNRS/ENS Lyon, Ecole Normale Supérieure de Lyon, 46 allée d'Italie, 69364 Lyon, France, <sup>2</sup>CGMC, UMR 5534 CNRS/Université Lyon-1 Claude Bernard, Bâtiment Mendel, 43 boulevard du 11 Novembre, 69622 Villeurbanne Cedex, France.

The nematode worm *Caenorhabditis elegans* was the first animal model whose genome was sequenced. However, many genetic mutations do not display any obvious morphological or behavioral phenotype under classical observations. We show that <sup>1</sup>H high-resolution magic angle spinning (HR-MAS) nuclear magnetic resonance spectroscopy is able to identify and quantify a large number of *C. elegans* metabolites. In this study, we present the first metabonomic protocol to obtain spectra of intact *C.elegans*. In association with biostatistics / chemometrics, we characterize metabolic fingerprints associated to genetic mutations. A metabonomic analysis, i.e. the hypothesis-free interpretation of biological NMR data by multivariate statistics, is particularly suited to understand pathophysiological perturbations in *C. elegans* mutants. Supervised multivariate statistics reveal a remarkable discrimination between the N2 strain (WT) and mutants of oxidative stress: SOD-1 mutants *sod-1(tm776)*, and Catalase-1 mutants *ctl-1(ok1242)*. We identify a metabolic phenotype (metabotype) significantly associated with these mutations: a general reduction of fatty acyl resonances from triglycerides, corresponding to a compensative strategy for regulation of oxidative stress. This work opens perspectives for the use of <sup>1</sup>H NMR HRMAS as a suitable molecular phenotyping device for *C.elegans* functional genomics.

ST-C-04

### NMR, EPR, and Kinetic Studies of the Structure and Function of the Alzheimer's Disease-Related Metallo- $\beta$ -Amyloid

Li-June Ming,<sup>1,2\*</sup> Alexander Angerhofer,<sup>3,\*</sup> Giordano da Silva,<sup>1</sup> and William Tay<sup>1</sup>

<sup>1</sup> Department of Chemistry, University of South Florida, Tampa, FL 33620,<sup>2</sup> Department of Chemistry, University of Florida, Gainesville, FL 32611,<sup>3</sup> Visiting professor at National Cheng Kung University and National Chung Hsing University, Taiwan

A tetragonally distorted octahedral metal coordination sphere with three coordinated His side chains and some specific H-bonding interactions are concluded from the electronic and EPR spectra of Cu<sup>II</sup>-A $\beta$ , hyperfine-shifted <sup>1</sup>H NMR spectrum of Co<sup>II</sup>-A $\beta$ , and molecular mechanics calculations. ESEEM (electron-spin echo envelope modulation) spectra of Cu<sup>II</sup>-A $\beta$  revealed the coordinated His side chains, coordinated water, and influence of Met. In addition, the Cu<sup>+2</sup> complexes of the Alzheimer's disease-related  $\beta$ -amyloid peptide (CuA $\beta$ ) and its 1-16 and the 1-20 fragments show significant hydroxylation/oxidation activities with enzyme-like kinetics toward a catechol and derivatives, phenol, and catecholamine neurotransmitters as well as oxidative plasmid DNA cleavage in the presence and absence of H<sub>2</sub>O<sub>2</sub>. A mechanism is proposed by the use of the catalytic cycle of dinuclear catechol oxidase as a working model.

In this catalysis, the substrate can bind and reduces the Cu<sup>2+</sup> center first, followed by O<sub>2</sub> binding to afford the  $\mu$ - $\eta^2$ : $\eta^2$ -peroxo intermediate which oxidizes a second substrate to complete the catalytic cycle, or through direct H<sub>2</sub>O<sub>2</sub> and substrate binding followed by oxidation of the substrate. This oxidative catalysis affords possible oxidative stress to biological macromolecules and supporting data to the pathological role of these soluble A $\beta$  fragments. This kinetic profile is consistent with metal-centered redox chemistry for the action of CuA $\beta$ . The results presented here are expected to add further insight into the structure and oxidative chemistry of metallo-A $\beta$  and the previously proposed role of Met35, and are expected to assist better understanding of the neuropathology of Alzheimer's disease.

ST-C-05

### Mechanism of ligand uptake and release in insect pheromone binding proteins

*Fred F. Damberger<sup>1</sup>, Erich Michel<sup>1</sup>, Yuko Ishida<sup>2</sup>, Walter S. Lea<sup>2</sup>, Kurt Wuthrich<sup>1,3</sup>*

<sup>1</sup>Institute for Molecular Biology and Biophysics, ETH Zürich, Zürich, Switzerland <sup>2</sup>Department of Entomology, University of California, Davis CA, USA, <sup>3</sup>Department of Molecular Biology and Skaggs Institute for Chemical Biology, The Scripps Research Institute, La Jolla, CA, USA.

The pheromone-binding protein from the silkworm, *Bombyx mori*, undergoes a pH-dependent conformational transition between the conformations BmorPBP<sup>B</sup>, which has a large hydrophobic cavity that can accommodate the natural ligand bombykol, and BmorPBP<sup>A</sup>, where the C-terminal tetradecapeptide segment of residues 129-142 forms a regular alpha-helix,  $\alpha$ 7, which inserts into the cavity and effectively blocks the ligand binding site [1-3]. The transition between BmorPBP<sup>B</sup> and BmorPBP<sup>A</sup> occurs near neutral pH in the absence of ligand, but is shifted to pH 5.5 in the presence of bombykol, indicating that bombykol competes with the helix  $\alpha$ 7 for the binding site. Moreover the intrinsic ligand "DTFP" which binds more tightly to BmorPBP than bombykol, shifts this transition to pH 5.3 and a truncated form of BmorPBP lacking the C-terminal tetradecapeptide is unable to release the ligand [4]. The C-terminal tetradecapeptide of BmorPBP has thus been recognized as a regulatory element in the functioning of the protein. Structural and NMR spectroscopic evidence for the unusual mechanism of ligand delivery in the moth pheromone-binding proteins will be presented to define the origin of the structural transition, and how the competitive equilibrium between the C-terminal tetradecapeptide and ligand for the binding cavity can contribute to the exquisite sensitivity and specificity of the olfactory system in silk moths.

ST-C-06

### Structural Basis for the Regulation of ASPP-Mediated Apoptosis of p53

*Jinwoo Ahn, In-Ja L. Byeon,\* Chang-Hyeock Byeon and Angela M. Gronenborn*

*Department of Structural Biology, University of Pittsburgh School of Medicine, Pittsburgh, PA 15260*

Recently, a new family of proteins, namely ASPPs (apoptosis-stimulating of p53 proteins), were discovered and found to regulate the apoptotic function of p53. ASPP1, ASPP2 and iASPP belong to this family and show high sequence homology at their C-termini, containing ankyrin repeats and a SH3 domain. These conserved C-terminal regions are responsible for the interaction with the DNA-binding core domain of p53. Despite of very similar sequences, ASPP1 and ASPP2 stimulate the apoptotic function of p53 whereas iASPP inhibits it. Furthermore it has been shown that iASPP binds to and regulates the activity of p53Pro72, a common p53 polymorphic variant, more efficiently than p53Arg72. This implies that the Pro-rich region of p53 is also involved in ASPP binding. The exquisitely balanced regulation of apoptotic activity most likely results from a subtle variation in binding modes within these complex systems. In order to understand the structural basis for the regulation of ASPP-mediated apoptosis, we embarked on a structural study involving the C-terminal fragments of ASPP1, ASPP2 and iASPP as well as p53 variants (both Arg72 and Pro72 versions) comprising the Pro-rich region and the core domain. We characterized the binding modes and strength of the p53-ASPP interactions by NMR, ITC and multi-angle light scattering methods. Our results show that ASPP2 binds p53Arg72 and p53Pro72 with similar affinities  $K_d \sim 1 \mu\text{M}$ , while ASPP1 and iASPP bind both p53 variants significantly weaker ( $K_d \geq 20 \mu\text{M}$ ). Binding site mapping by NMR on ASPP proteins revealed that ASPP2 interacts with p53 extensively through an extended binding

interface associated with large chemical shift changes. ASPP1 and iASPP exhibit fewer contacts with p53, accompanied by small shift changes. A detailed investigation of the involvement of the Pro-rich domain of p53 in the ASPP-binding and NMR structure determinations of the free ASPP and the ASPP/p53 complexes are currently being carried out.

**Oct. 16 11:45~12:15**

**ST-A-07**

### **19F NMR Characterization of Hemoproteins Reconstituted with Fluorinated Hemes**

Yamamoto Yasuhiko

*University Of Tsukuba, Japan*

NMR studies of hemoproteins such as myoglobin (Mb) and hemoglobin (Hb) in their various oxidation/ligation/spin states have provided a wealth of information on the electronic and structural properties of their active sites, which could offer substantial clues for delineating their structure-function relationships. Although  $^1\text{H}$  NMR studies of the active sites of hemoproteins are often hampered by the resolution of the signals, the introduction of fluorine atom(s) into specific site(s) of the proteins facilitates the observation of their NMR signals, owing to the absence of interfering background signals. Hence  $^{19}\text{F}$  NMR, combined with fluorinated hemes, readily provide useful spectroscopic information for the analysis of the heme electronic structure.

In this study, we characterized the structural and functional properties of oxy, carbonmonoxy, deoxy, and met forms of Mb using the  $^{19}\text{F}$  NMR technique. We demonstrated that the porphyrin  $\pi$ -system is affected by Fe  $d_{\pi} \rightarrow \text{CO } \pi^*$  back-donation in carbonmonoxy Mb and the bent orientation of the Fe-O-O unit relative to the heme in oxy Mb. We also found that the relative contributions of the putative orbital ground states, derived from  $^5\text{E}$ ,  $(d_{xz})^2(d_{yz})(d_{xy})(d_z^2)(d_{x^2-y^2})$  or  $(d_{yz})^2(d_{xz})(d_{xy})(d_z^2)(d_{x^2-y^2})$ , and  $^5\text{B}_2$ ,  $(d_{xy})^2(d_{xz})(d_{yz})(d_z^2)(d_{x^2-y^2})$ , states, to the heme electronic structure of deoxyMb are affected by the degree of the rhombicity of the porphyrin  $\pi$ -system exerted by chemical properties of the heme peripheral side-chains. Finally, we demonstrated that the thermodynamics and dynamics of the acid-alkaline transition in metMb can be characterized quantitatively using the present  $^{19}\text{F}$  NMR technique. Thus the present method is a new means of studying in detail structural properties relevant to functional regulation of various *b*-type hemoproteins to delineate their structure-function relationships.

**ST-A-08**

### **The INPHARMA Method as a Novel and Powerful Tool for Pharmacophore Mapping**

Julien Orts, Marcel Reese, Jennifer Tuma, Christian Griesinger, Teresa Carlomagno

*Max Planck Institute for Biophysical Chemistry, Department of NMR based Structural Biology, Am Fassberg 11, D-37077 Göttingen, Germany*

In structural based drug design knowledge of the orientation of the ligand in the receptor-binding pocket plays a central role in the elaboration of a high affinity drug. In this case it is desirable to develop a method that allows the determination of the ligand orientation (binding mode). Recently, we have developed a novel approach, called INPHARMA (Interligand Noes for PHARmacophore MApping), which allows the determination of the relative orientation of two competitive ligands in the receptor-binding pocket [1]. The method is based on the observation of interligand, spin diffusion mediated, transferred-NOE data, between two ligands A and B, binding competitively and weakly, to a macromolecular receptor T. During the mixing time of the NOESY experiment, the ligand A binds to the receptor and transfer the magnetization to the receptor proton, from  $H_A$  to  $H_T$ . Then ligand A dissociates from the protein and ligand B binds during the same mixing time of the NOESY experiment. The magnetization that was transferred from  $H_A$  to  $H_T$  is now transferred from  $H_T$  to  $H_B$  and leads to an intermolecular peak between  $H_A$  and  $H_B$ . Here, we compare the binding mode of two ligands derived from the INPHARMA method to the available crystal structures. Theoretical investigations of spin diffusion under chemical exchange are also presented. Previous studies, on spin diffusion, were done by R. E. London [2] and Feng Ni [3], based on a system in which the two

ligands bind non-competitively. Here we investigate spin diffusion and inter-ligand transfer NOE while the two ligands bind competitively and are never close from each other.

[1] V.M. Sanchez-Pedregal et al, *Angew. Chemie* 2005 44, 4172

[2] R. E. London, *JMR* 1999 141, 301-311

[3] Feng Ni, *Progress in NMR Spectroscopy*. 1994 26, 517-606

ST-B-07

### Local Structures and Dynamics of Phoborhodopsin and Transducer Leading to Signal Transduction as Revealed by Site-Directed Solid State $^{13}\text{C}$ NMR

*Akira Naito*<sup>1</sup>, *Izuru Kawamura*<sup>1</sup>, *Hideaki Yoshida*<sup>2</sup>, *Yoichi Ikeda*<sup>2</sup>, *Satoru Yamaguchi*<sup>3</sup>, *Satoru Tuzi*<sup>3</sup>, *Naoki Kamo*<sup>2</sup>, *Hazime Saito*<sup>4</sup>

<sup>1</sup>Yokohama National University, <sup>2</sup>Hokkaido University, <sup>3</sup>University of Hyogo, <sup>4</sup>Hiroshima University, Japan

Pharaonis phoborhodopsin (ppR) is a negative phototaxis receptor through complex formation with its cognate transducer (pHtrII) from *Natronomonus pharaonis*, leading to the photo-induced signal transduction. To understand molecular mechanism of the actions in archaeal rhodopsins, it is important to detect accurately the change of local structures and dynamics of protein side induced by the photo isomerization of retinal. Solid-state NMR is a powerful means to obtain information on the dynamic structure of membrane proteins in a biologically active state. We, therefore, examined  $^{13}\text{C}$  CP and DD-MAS NMR spectra of  $[3-^{13}\text{C}]\text{Ala}$  and  $[1-^{13}\text{C}]\text{Val}$ -labeled ppR, ppR(1-220) and D75N mutant (an presumed activated state) complexed with pHtrII, in order to reveal accompanied dynamics changes and a possible role of a C-terminal  $\alpha$ -helical region protruding from the cytoplasmic surface. It was revealed that the C-terminal  $\alpha$ -helix consisted of two regions, more static stem (Ala221) and flexible tip (Ala228, 234, 236 and 238) regions. The latter tip portion turns out to be participated in the complex formation. On the other hand, it turned out that the interaction between C-terminal and pHtrII become weaken when D75N was complexed with the transducer. These results indicate that the C-terminal  $\alpha$ -helix is involved in the photo-activated form of ppR-pHtrII complex as observed by solid-state  $^{13}\text{C}$  NMR. Subsequently, it turned out that pHtrII associates with each other to relay a signal to the further cytoplasmic regions after the photo activation. This finding gains insight into the signal relay pathway in the initial step of phototaxis receptor and its cognate transducer proteins.

ST-B-08

### Solid-State NMR Studies of the Structure and Dynamics of Membrane Bound Ras Proteins

*Guido Reuther*<sup>1</sup>, *Alexander Vogel*<sup>1</sup>, *Kui-Thong Tan*<sup>2</sup>, *Christine Nowak*<sup>2</sup>, *Jürgen Kuhlmann*<sup>2</sup>, *Herbert Waldmann*<sup>2</sup>, *Daniel Huster*<sup>1</sup>

<sup>1</sup>Junior Research Group "Structural Biology of Membrane Proteins", Institute of Biochemistry/Biotechnology, Martin Luther University Halle-Wittenberg, Kurt-Mothes-Str. 3, D-06120 Halle, Germany, <sup>2</sup>Max Planck Institute of Molecular Physiology, Dortmund, Germany

Covalent lipid modification is a common posttranslational event relevant for 5-10% of all proteins. In particular proteins involved in signal transduction are equipped with such a hydrophobic membrane anchor. By this mechanism, protein diffusion is constraint to two dimensions, which increases the probability to interact with downstream effectors. In spite of the biological significance of this mechanism, there is only little structural data available for lipidated proteins. Here, we show a model of the backbone structure of the membrane-associated lipid modified C-terminus of the full-length Ras protein determined by solid-state NMR. Functional Ras protein was obtained by bioorganic synthesis ligating the expressed water soluble N-terminus with chemically synthesized  $^{13}\text{C}$  labelled lipidated peptides. Complete assignment of the  $^1\text{H}$  and  $^{13}\text{C}$  NMR signals was obtained from correlation experiments. The calculated backbone structure of the membrane anchor of the Ras protein is based on the torsion angles determined from isotropic chemical shifts using TALOS. For the refinement of the structural model, additional correlation, nuclear Overhauser enhancement, and torsion angle experiments were carried out for a uniformly  $^{13}\text{C}/^{15}\text{N}$  labelled lipidated C-terminal heptapeptide representing the membrane anchor of the protein. Dynamical parameters for the lipid chain modification at Cys 181 were determined from static  $^2\text{H}$  NMR order parameter and relaxation measurements. Order parameters describing the amplitude of motion in the protein backbone and the side

chain were determined from site-specific measurements of  $^1\text{H}$ - $^{13}\text{C}$  dipolar couplings for all seven amino acids in the membrane anchor of Ras. The correlation times of motion were determined from temperature dependent relaxation time measurements and analyzed using a modified Lipari Szabo approach. Overall, the C-terminus of Ras shows a versatile dynamics with segmental fluctuations and axially symmetric overall motions on the membrane surface. In particular, the lipid chain modifications are highly flexible.

ST-C-07

## EPR Mapping of Inhibitor Binding Sites on Enzymes

Betty J. Gaffney<sup>1</sup>, Fayi Wu<sup>1</sup>

<sup>1</sup>Biological Science, Florida State University, Tallahassee, FL, USA

Spin labeled analogs of enzyme substrates allow EPR to be used in determining binding sites on enzymes that have not been crystallized in the presence of substrate. We have used spin labeled stearic acid derivatives as a means of probing the details of fatty acid binding sites in a lipoxygenase (LOX) and an allene oxide synthase (AOS) (Biochemistry 2006; 45: 12510-12518). Interestingly, the spin labeled stearates exhibit amplitudes of motion in the protein binding sites that depend on the label position on the stearate chain. 10-Doxyl stearate (10-DSA) is most rigidly bound in both LOX and AOS, although the proteins have highest affinity for 5-DSA. Both proteins contain paramagnetic iron, allowing estimates of the spin label-iron distances to be made. In new studies, site directed spin labeling is also employed with these enzymes to examine other distances between defined locations on the protein and the spin labeled substrate analogs. In particular, five sites around a suggested entrance to the lipoxygenase active site have been labeled with MTSL spin labels. Consistent with hypothesis, the two gating residues exhibit the most restricted motion of the attached spin label. In contrast, a suggested base for binding substrate carboxylate is not immobilized in the absence or presence of fatty acids, indicating that another site serves that role. Spin-spin interactions between the covalently attached MTSL and the doxyl group of the stearate substrate analogs are being examined at present with the aim of determining which end of the fatty acid substrate enters the binding site most deeply.

ST-C-08

## Multifrequency EPR Lineshape Analyses on Biradicals for High-Frequency Dynamic Nuclear Polarization

Kan-Nian Hu<sup>1,2</sup>, Changsik Song<sup>2</sup>, Hsiao-hua Yu<sup>2</sup>, Timothy M. Swager<sup>2</sup>, Robert G. Griffin<sup>1,2,\*</sup>

<sup>1</sup> Francis Bitter Magnet Laboratory and <sup>2</sup> Department of Chemistry, Massachusetts Institute of Technology, Cambridge, Massachusetts 02139, USA

To date the cross effect (CE) and thermal mixing (TM) mechanisms have consistently provided the largest enhancements in dynamic nuclear polarization (DNP) experiments performed at high magnetic fields (> 5 Tesla). Both the mechanisms involve a three-spin electron–electron–nucleus process whose efficiency depends primarily on two electron–electron interactions -- the interelectron distance,  $R$ , and the correct EPR frequency separation that matches the nuclear Larmor frequency,  $|\omega_{e1} - \omega_{e2}| = \omega_n$ . Biradicals, for example two TEMPO's (2,2,6,6-tetramethylpiperidin-1-oxyl) tethered with a molecular linker, can in principal constrain both the distance and relative g-tensor orientation between two unpaired electrons, allowing these two spectral parameters to be optimized for the CE and TM. To verify this hypothesis, we synthesized a series of biradicals -- bis-TEMPO tethered by  $n$  ethylene glycol units (BTnE) -- that show an increasing DNP enhancement with a decreasing tether length. Specifically, the enhancement grew from ~40 observed with 10 mM monomeric TEMPO, where the average  $R \sim 56$  Å, to ~175 with 5 mM BT2E (10 mM electrons) at 90 K and 5 T which has  $R \sim 13$  Å. In addition, we compared these DNP enhancements with those from three biradicals having shorter and more rigid tethers -- BTurea, BTOXA, and TOTAPOL. TOTAPOL which is of particular interest since it is soluble in aqueous media and compatible with DNP experiments on biological systems such as membrane and amyloid proteins. The interelectron distances and relative g-tensor orientations of all of these biradicals were characterized with analyses of their 9 and 140 GHz continuous-wave (CW) EPR lineshapes. The results from EPR experiments are consistent with the observation that larger DNP enhancements are observed with BT2E and TOTAPOL, which have shorter tethers and the two TEMPO moieties are oriented so as to satisfy the matching condition for the CE.

**Oct.17 11:45~12:15**

**ST-A-09**

**Large Pictures with Small Details: Combined Use of NMR and Scattering Data for RNA Structure Determination**

*X. Zuo<sup>1</sup>, J. Wang<sup>1</sup>, P. Yu<sup>1</sup>, C. Schwieters<sup>2</sup>, Y-X. Wang<sup>1</sup>*

*<sup>1</sup>PNAI, SBL, NCI-Frederick, NIH, Frederick, MD 21702, U.S.A.; <sup>2</sup>CBEL, CIT, NIH, Bethesda, MD 20892-5624, USA;*

In contrast to RNA's growing prominent roles in biological world, our knowledge base about the three-dimensional structures of RNAs is limited. This disparity is due to great difficulties in crystallizing RNA molecules suitable for diffraction or in determining the structures of functional size using solution NMR. We developed a combined approach to use NMR spectroscopy and scattering data, both of which are recorded in solution, for structure determination of large RNA molecules. NMR and scattering methods complement each other with information encompasses both local structural details and accurate global shape. In the combined approach, we use generic nucleic acids as building blocks, secondary, tertiary basepairings and chemical bond lineages as constraints to construct initial shape of molecules in order to interpret scattering data and to refine structure against the scattering and NMR restraints. This approach departs dramatically from the current field-wide popular bead-model approach to build up low-resolution molecular surface using beads based on scattering data. The combined approach also overcomes the difficulty in determining structures of large RNA molecules using only NMR due to lack of global order restraints. We demonstrate the utility of this approach in the structural determination of a 100-nt 3' UTR RNA, which plays a key role in regulation of gene expression.

**ST-A-10**

**Studies on the SARS coronavirus nucleocapsid protein using a hybrid approach – From structure to function**

*Chung-ke Chang<sup>1</sup>, Yuan-hsiang Chang<sup>1</sup>, Yen-lan Hsu<sup>1</sup>, Chun-Yuan Chen<sup>2</sup>, Ming-Chya Wu<sup>3</sup>, Chin-Kun Hu<sup>3</sup>, Chwan-Deng Hsiao<sup>2</sup>, and Tai-huang Huang<sup>1,\*</sup>*

*<sup>1</sup>Institute of Biomedical Sciences, <sup>2</sup>Institute of Molecular Biology, and <sup>3</sup>Institute of Physics, Academia Sinica, Taiwan*

The severe acute respiratory syndrome coronavirus (SARS-CoV) nucleocapsid protein (NP) binds to viral genomic single-stranded RNA and is required for virus viability. SARS-CoV NP consists of an N-terminal putative RNA-binding domain and a C-terminal dimerization domain connected together through a flexible linker. We employed a divide-and-conquer approach to study the biochemical and biophysical properties of the individual domains through NMR and various techniques and the use of single-stranded DNA (ssDNA) as RNA mimic. The N-terminal domain binds to ssDNA with low affinity and no specificity. Surprisingly, the C-terminal domain retains the ability to bind nucleic acid nonspecifically with apparently higher affinity than the N-terminal domain. Chemical shift disturbance studies indicate that two sites on the C-terminal domain participate in the binding event, with the second site coming into play only when the oligonucleotide is long enough. Electrophoretic mobility shift assays also show a slight base preference against poly(dA) for the C-terminal domain. Crystal structure analyses reveal a packing mode compatible with our current results and a helical packaging model. Interaction between the two domains and implications on nucleic acid binding will be discussed, including preliminary results from small-angle X-ray scattering studies of the di-domain construct.

**ST-B-09**

**Probing Amide Bond Nitrogens in Solids using <sup>14</sup>N NMR Spectroscopy**

*Sasa Antonijevic<sup>1</sup>, Nicholas Halpern-Manners<sup>1</sup>*

*<sup>1</sup>University of California Berkeley, USA*

A novel two-dimensional correlation nuclear magnetic resonance (NMR) experiment is proposed for

indirect observation of  $^{14}\text{N}$  nuclei in various types of nitrogen containing solids. In a method somewhat similar to the heteronuclear single-quantum correlation (HSQC) experiment widely used for protein structure determination in solutions, this technique correlates spin  $S = 1/2$  nuclei, e.g.,  $^1\text{H}$ ,  $^{13}\text{C}$ , with the  $^{14}\text{N}$  spin  $I = 1$  nucleus. The main difference is that the coherence transfer from neighboring  $^1\text{H}$  or  $^{13}\text{C}$  nuclei to  $^{14}\text{N}$  is achieved via a combination of J-couplings and residual dipolar splittings (RDS). Projections of the two-dimensional NMR spectra onto the  $^{14}\text{N}$  dimension yield powder patterns that reflect the  $^{14}\text{N}$  quadrupolar interaction, which can be used to study molecular structure and dynamics. Indirect detection of amide nitrogen-14 via  $^1\text{H}$  and  $^{13}\text{C}$  is shown experimentally on two model compounds: N-acetyl-D,L-valine and N-acetyl-glycine.

ST-B-10

### An *in situ* Solid State NMR Technique at Cryogenic Temperature

*Mingcan Xu<sup>1</sup>, Kenneth D.M. Harris<sup>1</sup>, John Meurig Thomas<sup>1,2</sup>, David E.W. Vaughan<sup>3</sup>*

*<sup>1</sup>School of Chemistry, Cardiff University, Wales, <sup>2</sup>Department of Materials Science and Metallurgy, University of Cambridge, Cambridge CB2 3QZ, England, <sup>3</sup>Materials Research Institute, Pennsylvania State University, University Park, PA 16802, U.S.A*

To overcome various disadvantages of existing *in situ* solid state NMR techniques, a straightforward and much simpler strategy is proposed to perform *in situ* solid state NMR experiment without any adaptation or modification of the NMR instrument. Here, the fast magic angle spinning (MAS) is exploited to “trigger” the *in situ* process. Probe molecules (liquid or solid) to be adsorbed are sealed in a thin-walled glass capillary tube avoiding contact with the sample. Both samples and capillary tube containing the probe molecules are put in the rotor. When start spinning, the large centrifugal force produced by the fast spinning breaks the capillary tube releasing probe molecules. Therefore, the adsorption process may start right in the spectrometer and an observation of the earliest stage of adsorption process is possible. In addition, a control of the temperature may help to slow down or accelerate the adsorption process. This *in situ* solid state NMR technique is ideal suitable for studies of adsorption processes of great interest in surface science and catalysis.

ST-C-09

### Spatial Effects in the Localised Detection of Coupled Metabolites *In Vivo*

*Richard AE Edden<sup>1</sup>, Peter B Barker<sup>2</sup>*

*<sup>1</sup>Cardif University, Wales, UK, <sup>2</sup>Russell H Morgan Department of Radiology and Radiological Sciences, The Johns Hopkins University, Baltimore, MD, USA*

*In vivo* human magnetic resonance scanners at higher field strengths (of 3T, 4T and 7T) yield sensitivity gains, allowing the quantitative detection of an increasing number of metabolites by magnetic resonance spectroscopy (MRS). Whereas traditional MRS has concentrated on the detection of singlets associated with NAA, Creatine and Choline, edited experiments, such as MEGA-PRESS, are now available to detect coupled spin systems, such as lactate, GABA, glutamate, glutathione and ascorbate. At high field strengths, with limited  $B_1$  field strength, the chemical shift artifact becomes large, and spatial variation in the phase of signals leads to signal cancellation. In this abstract, losses are considered in the detection of lactate by PRESS and of GABA and glutathione by MEGA-PRESS. Strategies to overcome the effects are demonstrated.

MEGA-PRESS, which has recently emerged as the most widely used editing experiment, is a difference experiment which relies on full evolution and refocusing of coupling in two experiments. Subtraction of the two removes all species which are unaffected by the editing pulse from the spectrum, leaving an edited difference signal from species of interest. Because the species to be detected are generally of low concentration and signal-to-noise is further diminished by splitting due to coupling, any increase in sensitivity which results from overcoming spatial effects has the potential to increase the number of practically detectable coupled compounds.

Complementary strategies to reduce spatial effects are discussed: high-bandwidth slice-selective

refocusing pulses; and the Inner-Volume Saturation (IVS) method. High-bandwidth pulses reduce the chemical-shift displacement, reducing the volume in which evolution of coupling is poorly behaved, leading to partial retrieval of the lost signal. IVS ensures that the evolution of coupling is well-behaved throughout the whole volume excited by first enlarging the excited volume and then suppressing the regions in which evolution is not optimal.

**ST-C-10**

### **Tract-Specific Analysis of Human White Matter: Mean-Path Based Method**

*W.-Y. CHIANG\*, H.-L. WANG, S.-C. HUANG, F.-C. YEH, W.-Y. TSENG*

*Center for Optoelectronic Biomedicine, National Taiwan University College of Medicine, Taipei, Taiwan*

Diffusion MRI has become an important tool for analyzing the microscopic property of neuronal fibers. Most of the current studies analyze diffusion indices such as mean diffusivity and fractional anisotropy (FA) within manually-defined regions of interest (ROIs). However, defining an ROI in a 3-dimensional volume is time consuming and subject to inter-observer variability. Although tract-based analysis can potentially ameliorate the above shortcoming, averaging the diffusion indices along the whole course of a fiber tract directly is subject to large variance because of the change of the indices along it. Moreover, for a specific tract bundle which is composed of multiple fiber tracts, defining the inter-tract correspondence is also a challenge. In this study, we proposed an automated algorithm to define the mean path of the fiber tracts within a bundle by averaging the local fiber directions and positions to overcome these problems. Fiber tracts within a fiber bundle intersected with the plane orthogonal to the mean path at each step were considered to be at the same path coordinates. Because no prior knowledge of corresponding points is needed for calculating mean path, this algorithm is generally applicable to fiber bundles of any curvature and more robust for thick and bending fiber bundles than existing methods. We applied this algorithm on healthy volunteers and patients with brain tumors and demonstrated the plots of diffusion indices along various fiber bundles including corticospinal tract, arcuate fasciculus, and corpus callosum. Using mean path, we show that there is  $20.5 \pm 9.5\%$  reduction of standard deviation of decomposed FA along arcuate fasciculus (9 participants) while there is not significant difference for cortical spinal tract (3 participants). Using the mean path as the coordinates for tract-specific analysis, we can detect subtle change of diffusion indices along a bundle to enhance the statistical differences in group comparison.

**Oct.18 11:45~12:15**

**ST-A-11**

### **Fast and Automated Assignment of ( $^1\text{H}$ - $^{15}\text{N}$ ) Amide Resonances of Proteins of Known 3D-structure.**

*Dirk Stratmann, Carine van Heijenoort and Eric Guittet \**

*ICSN, CNRS, Gif-sur-Yvette*

Structural genomic projects today yield an increasingly high number of proteins structures, mainly obtained by X-Ray diffraction, whose functions remain to be elucidated. NMR can play here a crucial role, through its ability to quickly identify binding sites of ligands or biological partners on proteins. An important NMR limiting step is the assignment of the HSQC spectra, which remains often fastidious for large proteins, and big efforts are being made to provide to the NMR community automated assignment methods. For proteins whose 3D structures are already known, structural NMR restraints like RDCs and  $\text{H}^{\text{N}}\text{-H}^{\text{N}}$  nOes, obtained from simple sensitive experiments, can be back-calculated from the structure. The matching of experimental and back-calculated data may then allow a straightforward assignment of HSQC spectra. In practice, the incompleteness and imprecision of the experimental restraints together with the discrepancies between reference and solution structures complicate the matching process. We propose here a new approach primarily based on  $^1\text{H}^{\text{N}}\text{-}^1\text{H}^{\text{N}}$  nOes. Contrary to most previously proposed methods, which search for a unique optimal assignment but which usually can't assess the correctness of the result, our program allows an exploration of all possible assignments compatible with experimental data. The procedure is fully automatic, and can be easily customized to include additional experimental restraint such as RDCs, or any

information about chemical shifts, amino acid type, accessibility, etc. We will show the result obtained on several proteins from XX to XX residues, using either synthetic or experimental data, and will analyze the amount and quality of experimental data needed to obtain a nearly unique assignment.

ST-A-12

### Automated NMR Structure Determination

*Torsten Herrmann, Pascal Bettendorff, Francesco Fiorito, Jochen Volk, Kurt Wüthrich*  
*ETH Zürich, Switzerland*

The presentation will focus on computational tools and protocols for automated three-dimensional structure determination by solution and solid state NMR.

For solution NMR, a fully automated protocol for structure determination of proteins will be presented. To this end, novel algorithms for automated backbone (MATCH) and side-chain resonance assignment (ASCAN) and an improved algorithm for automated NOESY peak picking and NOE assignment (RADAR) will be introduced. The application range and limitations of the fully automated protocol MATCH/ASCAN/RADAR will be discussed.

For solid state NMR, a modified version of the ATNOS/CANDID [1,2] algorithm for structural interpretation of two-dimensional proton-driven spin diffusion (PDS) correlation experiments will be presented. On the basis of model calculations, the present state of automated solid state NMR data analysis using ATNOS/CANDID will be discussed.

[1] T. Herrmann, P. Güntert and K. Wüthrich, *J. Mol. Biol.* **319**, 209-227 (2002)

[2] T. Herrmann, P. Güntert and K. Wüthrich, *J. Biomol. NMR* **24**, 171-189 (2002)

ST-B-11

### Structural and Functional Polymorphism of Chromodomains from Chromatin Remodeling Factors

*Yoshifumi Nishimura<sup>1</sup>, Masahiko Okuda<sup>1,2</sup>, Hideaki Shimojo<sup>1</sup>, Masami Horikoshi<sup>3</sup>*  
*<sup>1</sup>Yokohama City University, <sup>2</sup>Kihara Memorial Yokohama Foundation, <sup>3</sup>University of Tokyo, Japan*

Chromodomain, which is known as methylated histone H3 tail binding module, widely exists in many chromatin associated proteins. We have determined chromodomains from chromatin remodeling factors: histone acetyltransferase, Esa1 which is a catalytic subunit of the NuA4 complex, Esa1p-associated factor, Eaf3 which is a nonessential component of the NuA4 complex, and Chromo-Helicase/ATPase-DNA binding protein 1, Chd1 which is an ATP-dependent chromatin remodeling factor with two tandem chromodomains. In yeast Chd1, its binding ability to a K4 methylated histone H3 (H3 MeK4) is controversial. The second chromodomain (Cd2), but not the first chromodomain (Cd1) of yeast Chd1 was reported to bind dimethylated K4 on histone H3 directly. However, recent reports showed that a human homologue, CHD1 but not yeast Chd1 binds the H3 MeK4 by using tandem chromodomains and the complex structure was determined. We have solved solution structures of both Cd1 and Cd2 of yeast Chd1 and examined binding abilities of Cd1, Cd2, and a pair of Cd1 and Cd2. By detailed structural comparison with all chromodomains, we have identified two polymorphic regions, 1 and 2. Structural differences in the polymorphic region 2 revealed that both chromodomains of Chd1 have difficulty in adopting the methylated histone-binding mode as found in the chromodomains of the heterochromatin protein 1 and polycomb protein. Furthermore, large different structures in the polymorphic region 1 of CD1 between yeast Chd1 and human CHD1 obviously demonstrated that the chromodomains of yeast Chd1 can not be the H3 MeK4-binding module. These structural suggestions were verified by NMR perturbation experiments and surface plasmon analyses. We have concluded that the target of the chromodomains of yeast Chd1 is not the H3 MeK4 and other methylated histone tails.

## Solution Structures of DNA Duplexes Containing Oxidative Cytosine Lesions and Their Removal by DNA Glycosylases

*Varatharasa Thiviyathan*<sup>1</sup>, *Anoma Somasunderam*<sup>1</sup>, *David Volk*<sup>1</sup> *Tapas Hazra*<sup>2</sup>, *David Gorenstein*<sup>1,\*</sup>

<sup>1</sup>Sealy Center for Structural Biology, <sup>2</sup>Sealy Center for Molecular Sciences, University of Texas Medical Branch, Galveston, Texas 77555, United States.

Several studies have shown that the oxidized cytosine derivatives as the major chemical precursors for the GC to AT transition mutation, the most frequent point mutation in aerobic organisms. Among the oxidized cytosine products, 5-hydroxy uracil (5-OHU) shows the highest mutation potential. Using ab-initio calculations, UV spectroscopy and NMR methods, we have shown that 5-OHU can form stable base-pairs with all four DNA bases. Using NMR spectroscopy and restrained molecular dynamics, we have probed the detailed structures of DNA duplexes containing 5-OHU:X (where X= A, C, G or T) base-pairs. Phosphorus NMR shows that the presence of damaged residue alters the conformation and dynamics of the phosphate backbone of the duplexes, and such perturbations may contribute to target recognition by DNA repair enzymes. Our results explain why certain DNA polymerases preferentially incorporate G residues opposite 5-OHU, over the Watson-Crick base A. Among at least four human enzymes that are able to excise 5-OHU lesions from DNA duplexes, NEIL2 shows the highest activity. Using homology modeling, site-directed mutagenesis and spectroscopic methods, we have identified the DNA binding region of NEIL2, that forms a zinc finger motif. Homology modeling and proteolytic digestion showed that the 37kDa, 332-residue NEIL2 consists of two domains; a 134-residue C-terminal domain that consists of a conserved Zn-finger motif, and a 198-residue N-terminal domain. Our results showed that NEIL2 might be involved in transcription- and/or replication-coupled DNA repair. Structures of the N-terminal and C-terminal domains of NEIL2, determined by NMR spectroscopy, will be discussed. Our results show that the hydroxyl group in the 5<sup>th</sup> position of the 5-OHU residues would also serve as a marker recognized by the DNA repair enzyme.

## Quantum Oscillations in Photo-excited Triplet States in an External Magnetic Field

*Gerd Kothe*<sup>1</sup>, *Tomoaki Yago*<sup>1</sup>, *Michail Lukaschek*<sup>1</sup>, *Jörg-Ulrich Weidner*<sup>1</sup>, *Gerhard Link*<sup>1</sup>, *David J.*

*Sloop*<sup>2</sup>, *Tien-Sung Lir*<sup>2</sup>

<sup>1</sup>Department of Physical Chemistry, University of Freiburg, Albertstr. 21, D – 79104 Freiburg, GERMANY, <sup>2</sup>Department of Chemistry, Washington University, One Brookings Drive, St. Louis, MO 63130, USA

Quantum interference effects in photo-excited triplet states have attracted great interest since they probe fundamental aspects of the intersystem crossing process. In this study we explore the formation of quantum oscillations in photo-excited triplet states in an external magnetic field. Analysis reveals that pulsed light excitation initiates an oscillatory electron spin magnetization in the direction of the external field. The oscillation amplitude reaches a maximum when the electron Zeeman splitting matches the energy of a zero-field transition of the triplet state. This suggests that these quantum oscillations can be detected only at low magnetic fields. We report first successful low-field EPR experiments performed to validate the predictions of the model. In the presence of hyperfine interactions also quantum oscillations of nuclear spins are initiated. The analytical model shows that the amplitude of these nuclear coherences critically depends on the strength of the applied magnetic field. Generally, a maximum of the oscillation amplitudes is expected if the nuclear Zeeman frequency matches the hyperline coupling of a particular nucleus. Pulsed X-band EPR experiments, designed to probe these oscillations, are in good agreement with the predictions of the model. The formation of these nuclear coherences is associated with high nuclear spin polarization. For triplet pentacene in a p-terphenyl single crystal we observe an enhancement factor of  $P_z = 350$  even in a magnetic field of 1 Tesla. This might be relevant for structural and mechanistic NMR studies of proteins.

## A Low Temperature X-band Probe Head for Decoherence Time Study of Semiconductors

*N. Suwuntanasarn<sup>1</sup>, W. D. Hutchison<sup>1</sup>, G. Milford<sup>2</sup>, R. Bramley<sup>3</sup>*

<sup>1</sup>Centre for Quantum Computer Technology, School of Physical, Environmental and Mathematical Sciences, UNSW@ADFA, Canberra ACT 2600, <sup>2</sup>Centre for Quantum Computer Technology, School of Information Technology and Electrical Engineering, UNSW@ADFA, Canberra ACT 2600, <sup>3</sup>Research School of Chemistry, The Australian National University, Canberra ACT 2600

The design, numerical modelling, construction and performance of an X-band pulsed electron spin resonance (ESR) probe head is described. The probe head is specially designed to fit with an available Helium flow CW-ESR cryostat. The probe head main features include flexible matching and tuning capability and newly designed rectangular loop gap resonators (R-LGR), which are suitable for the semiconductor decoherence time study for quantum computing applications. The probe head geometry has been simulated and analysed numerically in detail by CST microwave studio suite. Three dimensional electromagnetic field aspects, conversion factor, quality factor and coupling coefficients are calculated and compared with the experiments. The agreement between the results provides a guide and validity for the use of the simulations as a tool for optimisation purpose. A homemade pulsed ESR system sensitivity assessment through noise figure analysis has been performed and evaluated. The pulsed ESR verification of the system is demonstrated through the decoherence time measurements on phosphorus doped natural silicon.

## Oct.18 15:10~16:10

## Alpha Hemoglobin Stabilizing Protein Sets a Conformational Trap to Stabilize Alpha Hemoglobin

*David A Gell<sup>1</sup>, Liang Feng<sup>2</sup>, Suiping Zhou<sup>3</sup>, Mitchell J. Weiss<sup>3</sup>, Yigong Shi<sup>2</sup> and Joel P Mackay<sup>1</sup>*

<sup>1</sup>School of Molecular and Microbial Biosciences, University of Sydney, NSW 2006 Australia; <sup>2</sup>Department of Molecular Biology, Lewis Thomas Laboratory, Princeton University, Princeton, New Jersey 08544, USA; <sup>3</sup>The Children's Hospital of Philadelphia and the University of Pennsylvania, Philadelphia, Pennsylvania 19104, USA

We have previously shown that alpha-haemoglobin stabilising protein (AHSP) protects developing red blood cells from the harmful effects of free alpha-globin. In the absence of its binding partner beta-globin, alpha-globin is an unstable protein that gives rise to damaging reactive oxygen species caused by reactions of the heme iron. AHSP forms an initial complex with oxy-alpha-globin and converts it over time to a stable and more inert low spin Fe(III) form in which the heme Fe is ligated at both of the reactive axial positions by histidine sidechains from alpha-globin.

We have studied the mechanism by which this conversion process occurs using a combination of NMR, X-ray crystallography and other biophysical methods. We conclude from our data that the initial binding event between AHSP and alpha-globin forces alpha-globin into a conformation that favours the loss of oxygen as superoxide – setting a kind of conformational trap. The loss of superoxide springs the trap and the presence of AHSP drives alpha-globin to form the stable bishistidyl Fe(III) form. We also find that the presence of a conserved proline in a specific position in AHSP fine tunes this protein for its role in stabilizing alpha-globin by favouring the formation of a cis-peptide bond in a critical alpha-globin binding loop.

## Protein Folding and ssDNA Binding of Cold-shock Protein CspB Studied on a nano-to-millisecond time

*Jochen Balbach<sup>1</sup>*

<sup>1</sup>University of Halle-Wittenberg, Institute of Physics, Biophysics group, D-06120 Halle(Saale), Germany

The cold shock protein CspB from *B. subtilis* binds to single stranded nucleic acids (ssDNA) [1-3]. Subtle differences in the structure of a CspB/ssDNA complex in solution [1] compared to the crystal structure [2,3] could be revealed. The analysis of the dynamics on a nano-to-picosecond time scale showed that an induced-fit mechanism underlies nanomolar binding of ssDNA. Global protein folding of CspB occurs on a millisecond time scale. Therefore, we used  $R_2$  dispersion measurements to study this folding reaction. Conventionally, fast protein folding rates are determined by optical stopped-flow methods (fluorescence or circular dichroism). We could determine the urea dependence of global unfolding and refolding rates on a residue-by-residue basis [4]. These data disclose a native-like transition state of folding for CspB. The observed millisecond dynamics of free CspB disappeared upon ssDNA binding.

[1] Zeeb, M., Max, K., Weininger, U., Löw, C., Sticht, H., Balbach, J. (2006). *Nucl. Acids Res.*, **34**, 4561-4571

[2] Max, K.E.A., Zeeb, M., Bienert, R., Balbach, J., Heinemann, U. (2006). *J. Mol. Biol.*, **34**, 4561-4571.

[3] Max, K.E.A., Zeeb, M., Bienert, R., Balbach, J., Heinemann, U. (2007). *FEBS J.*, **274**, 1265-1279.

[4] Zeeb, M., Balbach, J. (2005). *J. Am. Chem. Soc.*, **127**, 13207-13212.

**ST-A-15**

### **Kinetic and Equilibrium Intermediate Structures in Globin Proteins**

*Chiaki Nishimura, H. Jane Dyson, and Peter E. Wright*

*The Scripps Research Institute, La Jolla, California 92037, USA*

The folding of two globin proteins, apomyoglobin and apoleghemoglobin, was studied by pH-pulse labeling and interrupted H/D exchange with NMR detection in order to compare helical structure in their kinetic and equilibrium intermediates. NMR provides a powerful technique to obtain information about secondary structure formation in the transiently kinetic intermediate as well as the equilibrium intermediate, which is incompletely folded and flexible. For apoleghemoglobin, striking differences were observed between the equilibrium and kinetic intermediates. The helical structure of the kinetic intermediate, which is transiently observed after the initiation of the protein folding induced by a pH-jump, is composed of mainly G and H helices as well as partly E helix and CE loop regions. On the other hand, the equilibrium intermediate observed under slightly acidic conditions (pH ~ 4.0) contains the common G and H helices and less protected A and B helices. The former is quite consistent with the prediction plots of the average area buried upon folding based on the amino-acid sequences. These results suggest that the intermediate structure is so fragile that it is easily transformed depending on the solution condition, most likely pH, during the broad parallel pathway in the energy landscape.

Time-course studies during the protein folding of apoleghemoglobin revealed that, in the kinetic intermediate, non-native packing interactions are formed not only in the C-E loop region but also at the C-terminal end of each helix. There is an additional slow phase during the transition state of apoleghemoglobin folding, which is not observed in the apomyoglobin folding. These events, specific for apoleghemoglobin folding, are probably due to recovery from a non-native structure in the kinetic intermediate, including overall re-adjustment to form the native topology in the regions of the CE-loop and the C-terminal end of each helix.

**ST-A-16**

### **Structural Basis of Phosphor-counting Switch for Sequential Activation of a Checkpoint Kinase Cascade**

*Chunhua Yuan<sup>1</sup>, Hyun Lee<sup>2,4</sup>, Andrew Hammett<sup>5</sup>, Anjali Mahajan<sup>2</sup>, Chi-Fon Chang<sup>4</sup>, Jörg Heierhorst<sup>5</sup>, Ming-Daw Tsai<sup>1,2,3,4,\*</sup>*

<sup>1</sup>Campus Chemical Instrument Center, <sup>2</sup>Biophysics Program, <sup>3</sup>Departments of Chemistry and Biochemistry, The Ohio State University, Columbus, Ohio, USA <sup>4</sup>Genomics Research Center, Academia Sinica, Taiwan, <sup>5</sup>St. Vincent's Institute of medical Research, Fitzroy, Victoria, Australia

FHA domains and SQ/TQ cluster domains (SCDs) play important roles in DNA damage signaling. The

SCD1 (<sup>1</sup>MENIT<sup>5</sup>QPT<sup>8</sup>QQST<sup>12</sup>QAT<sup>15</sup>QRFLIE<sup>21</sup>) of yeast Rad53 has dual functions in regulating the activation of Rad53 and Dun1 kinases, which have one (Dun1-FHA) or two (Rad53-FHA1 and FHA2) FHA domains. The molecular mechanism behind this regulation is unknown. Our *in vivo* and *in vitro* studies show that SCD1 serves as an FHA domain-dependent phospho-counting switch for sequential activation of the Rad53-Dun1 checkpoint kinase cascade. Briefly, any single phosphothreonine of Rad53-SCD1 is sufficient for RAD53-dependent survival of replication fork stalling, but two adjacent phosphothreonines – pThr5 and pThr8 in particular – are necessary for Dun1 kinase activation. We proceeded to determine the Dun1-FHA structure in complex with a pThr-peptide derived from Rad53-SCD1 (<sup>3</sup>NI(pT)QP(pT)QQST<sup>12</sup>). The comparison with other FHA/pThr-peptide complexes, including the Rad53-FHA1/pThr5-peptide also solved here, clearly revealed similar binding region involving conserved (R60 and S74) and non-conserved (e.g. T75) residues in β3/β4, β4/β5, β6/β7, and β10/β11 loops/turns. However, in contrast to pTXX(D/I/L) short peptide recognition mode generally adopted by other FHA domains, (1) Dun1-FHA has two pThr binding sites, largely attributed to the existence of non-conserved R62 and R102; (2) β3/β4 and β4/β5 loops make comparatively more extensive contact to accommodate a longer peptide motif; (3) S11 makes considerable contribution to the binding. Taken together, the specificity for di-phosphorylated SCD1 peptide is conferred by three key determinants that constitute an optimal ligand motif pTXXpTXXS, which appears to be the extension of the “pT+3” rule. To a good approximation, they (pThr5, pThr8, and Ser11) are stabilized by the pair of R60 and R62, R102, and K129 in Dun1-FHA, respectively. In conclusion, this NMR study provides structural basis for a novel phospho-counting switch mechanism in signal transduction.

**ST-B-13**

### **High Resolution Solid-State <sup>1</sup>H-<sup>15</sup>N HETCOR Spectroscopy for Structural Characterization of Multiply-Labeled Peptides in Aligned Bilayers**

*Rigiang Fu<sup>1</sup>, Milton Truong<sup>2</sup>, Randy J. Saager<sup>3</sup>, Breanna S. Vollmar<sup>3</sup>, Timothy A. Cross<sup>1,2</sup>, Myriam Cotten<sup>3</sup>*

<sup>1</sup>National High Magnetic Field Laboratory; <sup>2</sup>Department of Chemistry and Biochemistry, Florida State University, Tallahassee, Florida 32310, USA. <sup>3</sup>Department of Chemistry, Pacific Lutheran University, Tacoma, Washington 98447, USA

Polarization inversion spin exchange at the magic angle (PISEMA), which correlates the orientation-dependent, anisotropic <sup>1</sup>H-<sup>15</sup>N heteronuclear dipolar couplings and <sup>15</sup>N chemical shifts, has been widely used for structural characterization of membrane proteins/polypeptides in ‘native-like’ lipid bilayers. PISEMA spectra from α-helices feature specific wheel patterns, which can be directly analyzed to obtain tilt, polarity, and high-resolution structures. So far, the orientational-dependent anisotropic <sup>1</sup>H chemical shifts, which provide complementary information for structural analyses including the hydrogen bonding geometry, have not been used for such structural characterization. Here, we use two-dimensional (2D) HETCOR spectroscopy to correlate the anisotropic <sup>1</sup>H chemical shifts and <sup>15</sup>N chemical shifts. We take advantage that when the <sup>15</sup>N decoupling is absent during the <sup>1</sup>H chemical shift dimension, the <sup>1</sup>H chemical shift resonances are split into two separated by the <sup>1</sup>H-<sup>15</sup>N heteronuclear dipolar couplings. Thus, the HETCOR spectra allow ones to obtain not only the <sup>1</sup>H-<sup>15</sup>N heteronuclear dipolar couplings and the <sup>15</sup>N chemical shifts as in PISEMA spectra, but also the <sup>1</sup>H chemical shift restraints from peptide planes.

In this presentation, we will demonstrate the advantages of the HETCOR method and its applications in the structural characterization of multiply-labeled Piscidin 1, p1, an Amphipathic Cationic Antimicrobial Peptide (ACAP) from the mast cells of fish. This 22 residue-long peptide is believed to play a crucial and direct role in the fight against many aquatic bacterial infections and it has been structurally analyzed from PISEMA data to be α-helical and oriented perpendicular to (~89°) the bilayer normal. Our detailed analyses of the HETCOR data from eight labeled sites reveal the presence of two helical segments separated by a small kink (~5°) at Gly13. This kink may be an indication of differences in the depth insertion of the antimicrobial p1 peptide in the hydrophobic bilayer from amino to carboxyl ends.

## Backbone Assignments in Solid-State Proteins using $J$ – Based 3D Heteronuclear Correlation Spectroscopy

Lingling Chen,<sup>1</sup> J. Michael Kaiser,<sup>1</sup> Tatyana Polenova,<sup>2</sup> Jun Yang,<sup>2</sup> Chad M. Rienstra,<sup>3</sup> and Leonard J. Mueller\*<sup>1</sup>

<sup>1</sup>Department of Chemistry, University of California, Riverside, California 92521, <sup>2</sup>Department of Chemistry and Biochemistry, University of Delaware, Newark, Delaware 19716, and <sup>3</sup>Department of Chemistry, University of Illinois at Urbana-Champaign, Urbana, IL 61801

Solid-state NMR spectroscopy is emerging as a mainstream tool in structural biology due to its unique capability to yield atomic-level information in macroscopically disordered systems. Resonance assignments are an essential first step in structural studies, and in the majority of studies to date, these have employed through-space, dipolar-driven correlation spectroscopy. Scalar-coupling-driven correlation in solids has been reported by several groups, but so far heteronuclear (<sup>13</sup>C, <sup>15</sup>N) scalar-based spectroscopy has not been demonstrated, despite its potential for improving backbone chemical shift assignment procedures. Here we show that heteronuclear 3D correlation experiments can be implemented using purely scalar based transfers. Specifically, 3D NCACO, NCOCA, and CANCO scalar-coupling driven correlation experiments are presented for protein backbone assignments in the solid-state. Using these  $J$  – MAS experiments, we find substantially increased spectral resolution without compromising sensitivity, which we find to be comparable to, or better than, that of dipolar methods. We illustrate this on three proteins, the  $\beta$ 1 immunoglobulin binding domain of protein G (GB1), reassembled thioredoxin (TRX), and the 140 kDa protein tryptophan synthase. Our results demonstrate that scalar-based methods are sufficiently well-developed to serve as a complementary tool to dipolar methods, which will be especially useful for the assignment of large proteins, where resonance overlap presents a major challenge to solid-state NMR.

## Enzyme Activation in Organic Solvents: Water Dynamics, Enzyme Dynamics, and Active Site Polarity via Solid-state NMR

Jeffrey A Reimer, Ross K. Eppler, Douglas S. Clark

Department of Chemical Engineering, University of California, Berkeley, Berkeley, CA USA

The direct coupling of protein dynamics to enzymatic turnover is strongly supported by convincing evidence that correlates dynamics and enzyme activity. Enzyme flexibility is hindered in organic solvents due to a decrease in the dielectric constant of the bulk solvent such that protein dynamics are significantly attenuated due to heightened electrostatic interactions. Coupled with the fact that proteins exhibit a wide dynamical range of motion depending on the specific solvent environment provides a unique opportunity to test the correlation between protein dynamics and enzyme activity. Towards that end we first employed <sup>2</sup>H NMR relaxation methods to examine the motion of enzyme-bound water for a series of enzyme-salt formulations in different organic solvents. These data provide indirect evidence that salt activation is mediated by increased water mobility. Moreover, we show that the presence of salt alters the local mobility of the enzyme-bound water in a manner similar to that of increasing temperature, thereby affording a greater degree of transition-state flexibility for the salt-activated biocatalyst over the salt-free biocatalyst. <sup>1</sup>H NMR relaxation measurements were then performed to specifically determine enzyme dynamics in three motional time regimes over a range of biocatalyst activities. These three time regimes were chosen to probe enzyme dynamics on the pico-second to tens of nanosecond timescale ( $T_1$  spin lattice relaxation), microsecond to millisecond regime ( $T_{1\rho}$  spin lattice relaxation in the rotating frame), and centisecond to second time regime ( $T_{1zz}$  longitudinal magnetization exchange). Active site polarity was investigated by monitoring the <sup>19</sup>F chemical shift of a fluorinated inhibitor located in the active site of SC. Our experiments reveal that activity strongly correlates with motions in the centisecond time regime, weakly correlates with motions in the millisecond regime, and does not correlate with protein motions on the pico, nano second time scale.

## Chemical Shift Analysis and Structural Studies of Human $\alpha$ -B Crystallin by MAS Solid-state NMR

*Stefan Jehle*<sup>1,2</sup>, *Ponni Rajagopal*<sup>3</sup>, *Hartmut Oschkinat*<sup>2</sup>, *Barth-Jan van Rossum*<sup>2</sup>

<sup>1</sup>Freie Universität Berlin, Germany; <sup>2</sup>Leibniz Institut für Molekulare Pharmakologie, Berlin, Germany; <sup>3</sup>University of Washington, Seattle, USA.

Solid-state magic-angle spinning (MAS) NMR spectroscopy extends structural studies to proteins that can not be assessed by other techniques like solution NMR and x-ray crystallography. However, structural studies of large biological systems like membrane proteins and heterogeneous oligomers still remain a challenge in structural biology.

We combine currently solid-state NMR and solution NMR (University of Washington, Seattle) to study the structure of human sHSP (small heat shock protein)  $\alpha$ -B crystallin. sHSPs prevent the aggregation of missfolded proteins and are involved in the cellular reaction to stress (e.g. heat, oxidation, pH). Especially ageing increases the incidence of diseases related with miss folded proteins like Alzheimer's disease and cataract in which  $\alpha$ -B crystallin plays a major role. The  $\alpha$ -B crystallin (175 residues, 20 kDa) is organized in three domains, the N-terminal domain, the core domain which has structural homology to other sHSPs and the C-terminal domain. The truncated core-domain can be studied by solution NMR, while the full length protein forms polydisperse large (600-800 kDa) oligomers that can be precipitated and studied by solid-state NMR. We expressed  $\alpha$ -B crystallin with various labelling schemes (uniformly-<sup>13</sup>C, <sup>15</sup>N and extensively-<sup>13</sup>C, <sup>15</sup>N labelled preparations). The latter were prepared by cell-growth on media containing 2-<sup>13</sup>C or 1,3-<sup>13</sup>C glycerol as sole carbon source.

We used liquid-state NMR assignments of the core domain as starting points for the solid-state NMR assignment of full length  $\alpha$ -B crystallin in the oligomer. Various 3D MAS NMR spectra of the three differently labelled protein preparations were recorded and used in a self-consistent sequential assignment. From these data we could assign ~70% of the full length  $\alpha$ -B crystallin whilst the core domain itself has been assigned almost completely. Several long range correlations implicate the secondary structure of the core domain in the oligomer. Additional chemical shift analysis and comparison with solution NMR shifts provide information of probable interaction sites in the oligomer.

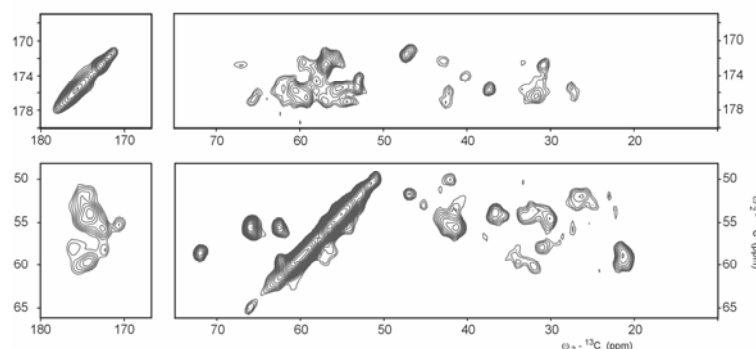


**Figure:** <sup>13</sup>C-<sup>13</sup>C planes extracted from a 3D MAS NMR NCOCX (top) and NCACX (bottom) experiments, recorded from uniformly-<sup>13</sup>C, <sup>15</sup>N-labelled  $\alpha$ -B-crystallin. The spectra were recorded at 700 MHz <sup>1</sup>H frequency.

## Enhancement of Spin Diffusion of Quadrupolar Spins in Solids under Magic-Angle-Spinning

*Po-Chi Huang*, *Shangwu Ding*

Chemistry Department, National Sun Yat-Sen University, No.70, Lianhai Rd., Gushan District, Kaohsiung City 804, Taiwan(ROC)

MQMAS and STMAS have become an indispensable tool in solid state NMR. A regrettable fact for these methods is that only the (two) principal components of the EFG tensor for each quadrupolar nucleus can be elucidated from the spectrum. The other, equally important, parameters, i.e., the three components determining the orientation of the tensor with respect to a fixed frame, are inaccessible. When extended to spin-diffusion type experiments, the cross peaks between two quadrupolar spins contain information about these remaining three components and simulation of the 2D lineshape of these peaks can provide the values of these components with good accuracy. Unfortunately, these cross peaks are normally very weak and their lineshapes are not good enough to guarantee accurate determination of the tensor orientation.

The reasons are: weak dipolar couplings (either mediated by hydrogen or direct coupling) and averaging effect of sample spinning. In this work, we report the results on enhancing the cross peaks by recoupling quadrupolar spins through pulsing hydrogen and/or quadrupolar spins during mixing time. Tests on a number of systems show that the enhancing effect is encouraging and the quality of the cross peaks can be improved so that accurate elucidation of the relative orientation of quadrupolar spin pairs can be achieved on typical compounds.

**ST-C-14**

### **MRI Signal Enhancement in Rodent Brain by Pulmonary Infusion of MnCl<sub>2</sub>**

*Kyuhong Lee<sup>1</sup>, Hye-Young Moon<sup>1</sup>, Hong-il Lee<sup>1</sup>, Chaejoon Cheong<sup>1</sup>, Kwan Soo Hong<sup>1</sup>*

<sup>1</sup>MRI Team, Korea Basic Science Institute, Ochang,

Recently 'manganese enhanced MRI (MEMRI)' has been applied to various studies on brain anatomy and function. It uses that the magnetic local moments of Mn<sup>2+</sup> ions give MR signal enhancement from T<sub>1</sub> shortening effect of water protons in tissues with making T<sub>1</sub> weighted image contrasts. Brain MRI researches are to be performed using the fact that Mn<sup>2+</sup> ions are uptaken through voltage gated calcium channels [1]. In MEMRI, the infusion method of Mn<sup>2+</sup> into animal body is very important experimentally. In literature two kinds are shown. One is a direct injection into specific region in animal brain with MnCl<sub>2</sub> solution. MnCl<sub>2</sub> administrations into vitreous body of the eye for retinal projection mapping are reported. The other is a systemic infusion like intra-peritoneal (IP), intravenous (IV), and subcutaneous (SC) [2][3]. Many researches using these routes have been reported. But these have a serious problem of unexpected animal death during experiments.

In this study, we suggest so called 'pulmonary infusion (PI)' as a new route to delivery Mn<sup>2+</sup> ions to animal system for MEMRI. Infusion of Mn<sup>2+</sup> into system through lung, we can be achieved with the MRI signal enhancement in the rodent brains. This is totally different and new method compared with the conventional systemic administration of MnCl<sub>2</sub> solution. The instillation through trachea is recruited to infuse Mn<sup>2+</sup> into animal system. We made comparative study between this new Mn ions infusion route and conventional systemic injection, IP. LD50 for PI was measured in the way of OECD guideline for testing of chemicals. PI below LD50 has made no unwanted animal death.

This work was supported by the 21th Century Frontier R&D Program (CBM2-B611-001-2-1-0) from the Center for Biological Modulators and by the Bio-MR Research Program (E27070) from the Korean Ministry of Science and Technology.

**ST-C-15**

### **<sup>13</sup>CO<sub>2</sub> labeling into plant biomass and its bacterial degradation followed by solution and solid-state NMR**

*Jun Kikuchi<sup>1,2,3</sup>, Tetsuya Mori<sup>4</sup>, Masahiro Yuki<sup>4</sup>, and Takashi Hirayama<sup>3,4,5</sup>*

<sup>1</sup>RIKEN Plant Science Center, JAPAN; <sup>2</sup>Grad. Sch. Bioagri. Sci., Nagoya Univ., JAPAN; <sup>3</sup>CREST, JST., JAPAN; <sup>4</sup>Int. Grad. Sch. Arts Sci., Yokohama City Univ., JAPAN; <sup>5</sup>Environ. Mol. Biol. Lab., RIKEN, JAPAN

Since plants can be fixing CO<sub>2</sub> into their useful biomass such as cellulose and starch, studies of their carbon dynamics is important field in the era of post petrol industry. The NMR-based metabomics approach has much potential to follow plant carbon fixation, biomass synthesis and degradation. Firstly, 1D-<sup>1</sup>H-NMR metabolic fingerprinting can be used for characterization of cell-wall mutants of *Arabidopsis* and *Populus*. Identification of changed metabolites would be performed by multi-dimensional NMR coupled with stable isotope labeling of plants (1-4) and by use of our original Java software, SpinAssign and original standard database. In addition to this, the uniform <sup>13</sup>C labeling can be used in metabolic flux analysis of plant samples at atomic level (5). Furthermore, we have observed nicely resolved <sup>1</sup>H-<sup>13</sup>C cross peaks of non-extracted, insoluble small and macromolecules by magic-angle-spinning NMR experiments. Especially, the solid-state NMR studies can be used to characterize structure and dynamics of <sup>13</sup>C-plant biomass. Finally, the <sup>13</sup>C-cellulose was purified from the <sup>13</sup>C-labeled plant and it was fed with the termite for two weeks. The degradation of the <sup>13</sup>C-cellulose by symbiotic bacteria was followed by our NMR-based metabomics approach. Usefulness of uniform <sup>13</sup>C-labeling of plants and their characterization by solution and solid-state NMR

will be discussed in the conference.

<References>

- (1) Kikuchi, J., Shinozaki, K. & Hirayama, T. *Plant Cell Physiol.* **45**, 1099-1104 (2004).
- (2) Kikuchi, J. & Hirayama, T. *Biotech. Agri. Forest.* **57**, 93-101 (2006).
- (3) Kikuchi, J. & Hirayama, T. *Method Mol. Biol.* **358**, 273-286 (2007)
- (4) Tian C.J., Chikayama, E., Tsuboi, Y., Kuromori, T., Shinozaki, K., Kikuchi, J. & Hirayama, T. *J. Biol. Chem.* (in press).
- (5) Sekiyama, Y & Kikuchi, J. *Phytochemistry* (in press).

**ST-C-16**

### **Study of Long-Term Stability of Yttrium-Iron Garnet Films under Irradiation by Reactor Neutrons**

V. A. Ageev<sup>1</sup>, V. I. Kirischuk<sup>1</sup>, Yu. V. Koblyanskiy<sup>2</sup>, G. A. Melkov<sup>2</sup>, L. V. Sadovnikov<sup>1</sup>, N. V. Strilchuk<sup>1</sup> and V. A. Zheltonozhsky<sup>1</sup>

<sup>1</sup>Institute for Nuclear Research, National Academy of Sciences, Kiev, Ukraine; <sup>2</sup>Taras Shevchenko National University, Kiev, Ukraine

Oscillations and waves of magnetization (or spin waves) in Yttrium-Iron Garnet (YIG) ferrite films and mono-crystals have very interesting and useful properties that can be used for the development of novel nonlinear microwave signal processing devices based on the parametric interaction of spin wave packets propagating in the films with localized electromagnetic fields of microwave pumping. So it is very important to develop a simple and reliable method to control and modify the structure and properties of YIG ferrite films and mono-crystals at nano-scale.

In our present work we provide experimental evidence demonstrating that irradiation of single crystal ferrite films and bulk ferrite samples with reactor neutrons leads to the increase in the number of nano-sized defects in these materials and their ferromagnetic resonance (FMR) linewidth broadening that is directly related to the number of the magnetic nano-sized defects.

Four YIG samples, each presenting a YIG ferrite film of 5  $\mu\text{m}$  thickness at gallium-gadolinium garnet undercoat of 500  $\mu\text{m}$  thickness, were irradiated by reactor neutrons up to the fluences of  $3.7 \times 10^{17}$  n/cm<sup>2</sup>,  $1.6 \times 10^{18}$  n/cm<sup>2</sup>,  $6.2 \times 10^{18}$  n/cm<sup>2</sup> and  $1.5 \times 10^{19}$  n/cm<sup>2</sup>, respectively. The neutron fluence accumulated by every YIG sample has been controlled using long-lived nuclides activated by thermal and fast neutrons during the irradiation. The investigation of YIG samples has shown that FMR lines did broaden by 11%, 41%, 320%, and 660%, correspondingly.

As a result, ferrite devices have surely higher long-time stability in comparison with traditional semiconductor ones allowing them to be used in modern radar technologies, space communication systems and other microwave equipment that should be able to withstand high radiation levels. At the same time, parameters and properties of YIG ferrite films and microwave ferrite devices that use such films can simply and reliably be controlled and changed at nano-scale.